Mn-Fe-Enhancing Budding Bacteria in Century-Old Rock Varnish, Erie Barge Canal, New York

David H. Krinsley,[1] *Barry DiGregorio,*[2] *Ronald I. Dorn,*[3,*]
Josh Razink,[4] *and Robert Fisher*[4]

1. Department of Geological Sciences, University of Oregon, Eugene, Oregon 97403, USA; 2. Buckingham
Centre for Astrobiology, University of Buckingham, Buckingham MK18 1EG, United Kingdom
3. School of Geographical Sciences and Urban Planning, Arizona State University, Tempe,
Arizona 85287-5302, USA; 4. Center for Advanced Materials Characterization in
Oregon (CAMCOR), University of Oregon, Eugene, Oregon 97402, USA

ABSTRACT

Fossil remnants of bacteria involved in the enhancement of manganese and iron rarely occur within the microstratigraphy of rock varnishes collected from warm desert environments, because varnish formation processes ultimately destroy these microfossils through remobilization of Mn-Fe and reprecipitation in a clay-mineral matrix. In contrast, Mn-Fe encrustations on budding bacteria commonly occur within varnishes that formed within just a century along the Erie Barge Canal, New York. Nanoscale imagery and elemental analyses reveal that these budding bacterial forms greatly enhance Mn, Fe, or both in encrustations surrounding hyphae and cells. The Mn and Fe precipitates have a granular texture on the scale of <1 nm to ~10 nm. The precipitates also have a stringy texture, where strings are typically only a few nanometers wide. These in situ observations are consistent with expectations from studies of budding-bacteria cultures and with the polygenetic model of varnish formation. Given that the Erie Canal site presents the fastest known rate of varnishing, with typical thicknesses around 15 μm formed in a century, only one or two budding bacteria encrusting Mn-Fe oxides each year would be sufficient to generate the observed Erie Canal varnish. This contrasts with one bacterium growing every ~400 y being needed to generate observed rates of varnishing in typical warm desert settings.

Introduction

Aristovskaya (1961) described two species of budding bacteria able to enhance manganese and iron. Hirsch and Conti (1964) then examined budding and hyphae-producing bacteria (Labrenz 2004). One of budding bacteria's characteristics noted by Aristovskaya, Hirsch, students, and colleagues involves encrustation of cells with manganese and iron oxides (Aristovskaya and Zavarzin 1971; Aristovskaya and Hirsch 1974; Hirsch 1974; Ghiorse and Hirsch 1979; Ghiorse 1984; Hirsch et al. 1995). Certainly, budding bacteria are not the only type of bacteria or fungi able to oxidize and enhance manganese (Nealson and Tebo 1980; Tebo et al. 2004, 2005; Nealson 2006), but budding bacteria are the focus of this study because genera such as *Hyphomicrobium* and *Pedomicrobium* can continue to grow away from Mn and Fe encrustation by budding cells from their hyphae (Aristovskaya 1963; Tyler and Marshall 1967*a*, 1967*b*; Tebo et al. 2005; Braun et al. 2009).

Budding bacteria able to precipitate manganese and iron oxides grow on rock varnishes found in warm deserts, as noted through in situ observations using a combination of secondary electron (SE) imagery and energy-dispersive spectroscopy of X-rays (EDS; Krumbein 1969; Dorn and Oberlander 1981*a*, 1982; Krumbein and Jens 1981). Budding bacterial forms concentrating Mn and Fe on rock varnishes also occur in cold desert settings such as Tibet (Krinsley et al. 2009; Wang et al. 2011), in Italy (Esposito et al. 2015), and along tropical rivers (Dorn et al. 2012; Keim et al. 2015). In situ observations also reveal that budding bacteria produce Mn-rich

deposits on rocks in such varied environments as mountain soils (Khak-mun 1966, 1968), acid mine drainage (Tebo et al. 2005), and caves (Northrup et al. 2003; Lozano and Rossi 2012). Culturing studies indicate the presence of budding bacteria *Pedomicrobium* sp. and *Metallogenium* sp. (Dorn and Oberlander 1981*a*, 1982), a new species of *Pedomicrobium* (Taylor-George et al. 1983), and a prostate budding bacterium similar in morphology to *Hyphomicrobium-Hyphomonas* sp. (Palmer et al. 1985), and *Geodermatophilus* sp. has been sequenced, can express a budding form (Ivanova et al. 2010), and occurs in association with Mn oxidation in varnish (Hungate et al. 1987).

The occurrence of microbial fossils of budding bacteria within varnish microstratigraphy, however, has not been reported previously. In general, microfossils within varnish layers typically remains quite rare in warm deserts (Dorn 1998, 2009; Dorn and Krinsley 2011), because ongoing diagenesis mobilizes the Mn and Fe from the casts of bacterial cells. The Mn-Fe then moves into clay structures (Dorn 1998, 2007; Krinsley 1998; Krinsley et al. 2013). Anomalously fast-growing varnishes, such as those found at the Fontana slag site in California, in contrast, contain an abundance of Mn-encrusted microfossils within varnish (Dorn and Meek 1995).

The general significance of microbial enhancement of Mn and Fe rests in a possible explanatory mechanism for high concentrations of Mn-Fe oxides found in rock (or desert) varnish (von Humboldt 1812; Linck 1900; Lucas 1905; Basedow 1914; Engel and Sharp 1958; Dorn and Oberlander 1982). The main contribution of this article rests in presenting the first in situ evidence of budding bacterial forms observed directly enhancing both Mn and Fe inside varnish stratigraphy, using nanoscale electron microscope imagery and chemical analyses. A key to this study is the natural laboratory of very rapid varnish formation at an Erie Barge Canal study site in New York, where rock varnish completely coats quarried sandstone in a century.

Study Site

Prior initial research into the nature of Mn-rich rock coatings in New York identified an area along the Erie Canal as a site of varnish growth within a century (Krinsley et al. 2012). The sample(s) collected for further study on November 25, 2014, came from a fine-grained red Medina sandstone weighing approximately 9 kg and measuring 30.4 cm × 22.8 cm × 5.1 cm (fig. 1*A*). The clast is at the top of the north bank on the Erie Canal Heritage Trail in Holley, New York (43.254482°N, 78.079211°W).

The area has a humid continental climate heavily influenced by both Lake Erie and Lake Ontario, where between 710 and 1600 mm of precipitation falls annually. Western New York is known for its lake-effect snows, usually most active between November and February, that can result in highly localized intense snow events. Average annual lake-effect snows exceed 380 cm downwind of Lake Erie and 510 cm downwind of Lake Ontario. Average annual cloud cover is 71%–75%.

The Erie Canal runs from east to west across most of New York State, 584 km from Albany to Buffalo, having a north bank and a south bank. The sampled north bank of the canal is the original tow path used by early merchants, who had large barges loaded with goods that were "towed" by mules or horses. With the advent of steam-powered boats, wave wash eroded the tow path and damaged the canal clay bed. By 1905 a canal expansion project, authorized by the New York State Legislature, utilized steam and later diesel tugs and replaced the old Erie Canal in 1918 (Percy 1993).

Both banks of the larger canal were then lined with 25–30-cm boulders that included the Medina sandstone, granite, and limestone. Annual dredging operations still ongoing to this day by canal maintenance workers use excavators (fig. 1*D*) to reclaim riprap that tumbles to the bottom of the canal. This dredging is done during winter months, when the canal is drained of most of its water (fig. 1*B*). Clay and silt at the bottom of the canal are also pulled up with the reclaimed riprap and placed back into the areas from where it had fallen from the banks. The majority of the varnished sandstone and some granite rocks occur about 1.5 m above the canal water line on a limited section approximately 55 cm wide at the top of the north bank. Rocks below this level and going to the water line appear relatively free of varnish, perhaps related to frequent soakings from the waves caused by passing boats. Another factor related to dredging operations could be the placement of dredged clays (fig. 1*D*) on sandstone surfaces (fig. 2), since clays are known to be a key component of varnish accretionary processes (Potter and Rossman 1977; Dorn and Oberlander 1982; Krinsley et al. 1995; Israel et al. 1997; Krinsley 1998; Diaz et al. 2002; Probst et al. 2002).

Field surveys of the Erie Canal from Lockport to Holley, New York, revealed the presence of rock varnish on many of the sandstone and granitic rocks on the north bank (fig. 1*C*), although limestone clasts lack varnish. The red and gray sandstones derive from a quarry in the Medina Group of the lower Silurian (Duke 1991; Brett et al. 1995). When these fine-grained red and gray Medina sandstone
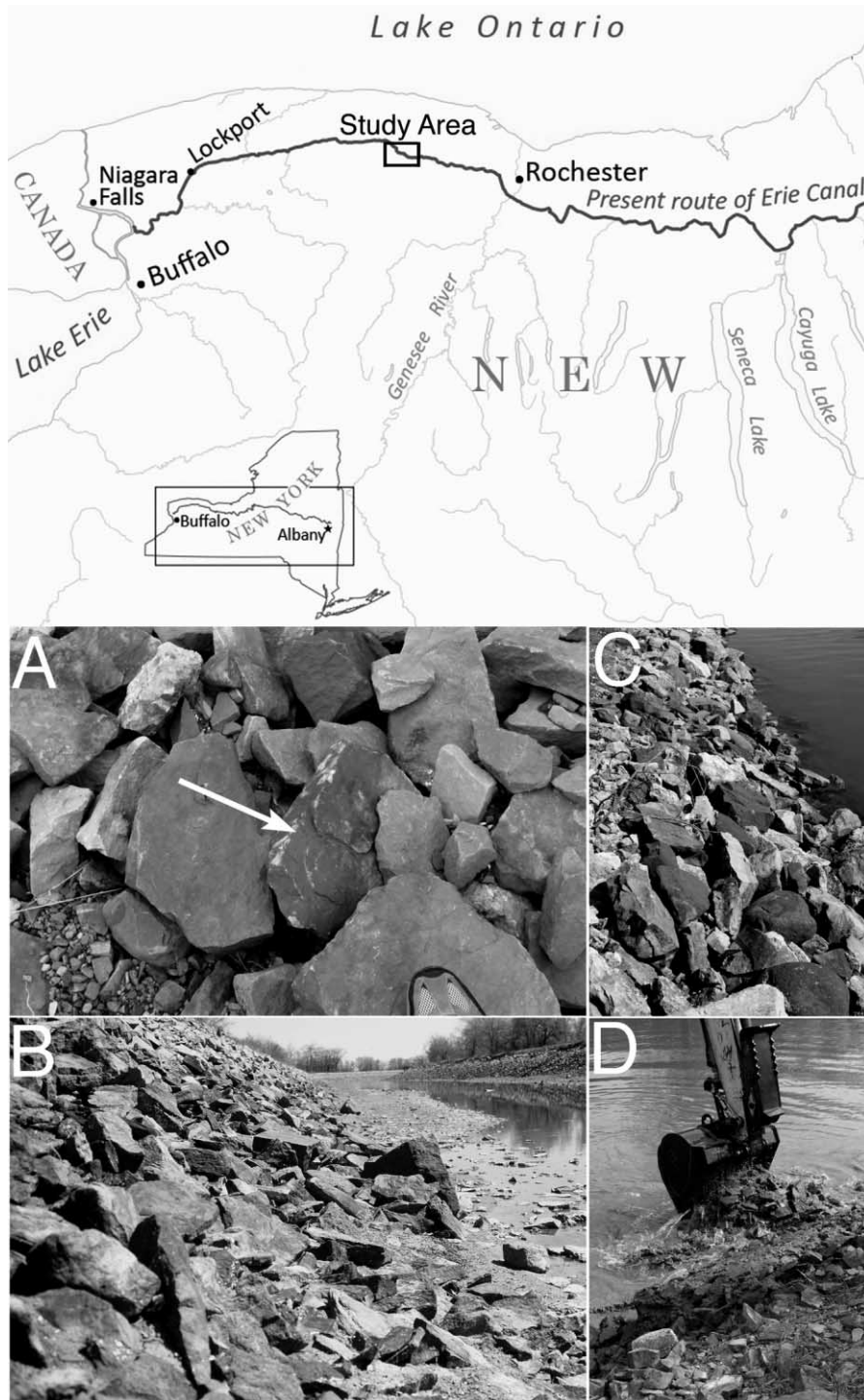
Figure 1. The study area is between Lockport and Rochester along the Erie Canal, where the base map is the USGS National Map. *A*, Varnished red sandstone boulder (arrow) selected for sampling. *B*, Wintertime view of riprap that has fallen to the bottom of the drained canal and will be dredged up before the spring boating season begins. *C*, Summer view of a varnished sandstones intermixed with unvarnished limestone riprap near the top of the canal. *D*, Erie Canal dredging of riprap and the thick layer of clay and silt mixed in with the reclaimed riprap. A color version of this figure is available online.
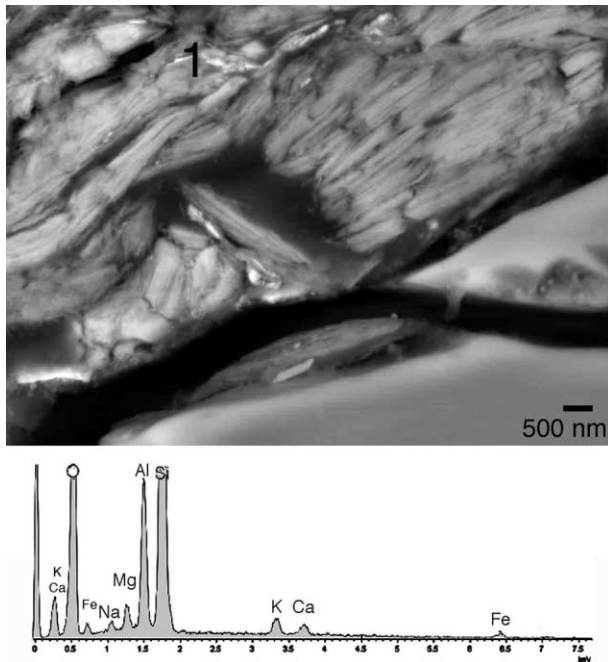
Figure 2. The dredged-up, unconsolidated sediment resting on the surfaces of quartz consists of clay-sized particles in discrete "pods" that are typically a few microns in length and a few hundred nanometers in thickness, seen in this back-scattered electron image. These laminar materials resemble clay minerals in their texture and energy-dispersive spectroscopy elemental spectra, as exemplified by an analysis at the position labeled 1.

rocks were originally hand-drilled and blasted out from local quarries in the early twentieth century (with most quarries abandoned by 1920), they were graded either as building stones or for use as riprap along the banks of the canal. All the rock material graded for use as riprap was originally hand-placed on the banks by Erie Canal workers working from barges.

Varnishing could have started immediately after quarrying or well after quarrying, because it is distinctly possible that the process of clasts falling down into the canal, followed by dredging, allowed Mn/Fe oxidizers that could have originated in the canal waters to inhabit rock surfaces while they were inundated. Thus, the maximum age of the Erie Barge Canal varnishes would be a century. The minimum age would be sometime before 2012, when the second author initiated field observations.

Riprap on the north-facing south bank of the Erie Canal does not host rock varnish. Sandstone blocks in the quarries abandoned in the 1920s similarly do not show any varnish development, and these quarry exposures also face north. The lack of varnish devel-

opment in these more mesic settings could be due to greater competition from lithobionts such as fungi, algae, and moss that prefer the greater moisture abundance that shaded locations offer.

Today all of the various rocks making up the riprap lining the banks of the Erie Canal have some degree of microbial weathering, with colonies of cyanobacteria, fungi, lichens, and iron films apparent to the naked eye. Canal maintenance workers today replace old riprap with only dolomite, while sandstone riprap fell out of use after the sandstone quarries were abandoned by 1920. This makes the Erie Canal a candidate for geomicrobiology studies of in situ lithobiontic communities that can be dated to within a century where a combination of quarried sandstone, granite, and limestone were originally used as riprap to line the canal banks against erosion.

Methods

The process of sample preparation for imaging with scanning transmission electron microscopy (STEM) and analysis with EDS starts with a polished cross section observed with SE and back-scattered electron (BSE) microscope imagery. The second stage of sample preparation involves making cuts with a dual-beam focused ion beam (DB-FIB) to allow the in situ Omniprobe device (Ditto et al. 2012) to manipulate samples. The third stage involves thinning with the DB-FIB to make the sample thin enough to transmit the electron beam and image in STEM. We used an FEI 80–300-kV Image-Corrected Titan equipped with a 30-mm^2 EDAX X-ray detector.

The EDS analyses of multiple points in different locations around a thinned sample allow a semi-quantitative understanding of elemental variations. Most of the peaks in the EDS spectra are artifacts associated with sample preparation—from Cu in the TEM grid, Ga and Pt are involved in sample preparation. The porous and heterogeneous nature of varnish does not allow a strict quantitative determination of elemental mass percentages within the sample. Quantitative analysis requires the use of samples with equivalent working distance, accelerating voltage, sampling volume, surface characteristics, back-scattering efficiency, electron stopping power, and characteristics of X-ray absorption and secondary fluorescence (Richie 2013) and not only would account for matrix effects but also would include the use of internal or external standard calibration procedures, quantification or control for background, sensitivity coefficients, and binary influence coefficients from matrix effects (de Vries and Vrebos 2002; Skoog et al. 2007). However, EDS can

record semiquantitative and relative trends in elemental composition across the sample, allowing a reasonable comparison Mn and Fe in EDS spectra. To aid in reader interpretation, we add annotations to the EDS spectra so that the major peaks can be identified more easily.

Results

Figure 3 and table 1 present a micron-scale overview of a typical area of rock varnish observed at the Erie Canal study site. Note that Mn and Fe are fairly evenly distributed throughout this varnish cross section, as revealed by the EDS dot maps (fig. 3*B*, 3*C*). In the semiquantitative EDS analyses, Mg-Al-Si abundance is consistent with the presence of clay minerals as a binding agent, even though Mn and Fe are in greater abundance than is found in typical warm, arid varnishes (Dorn 1998). Table 1 reveals that lead is present at concentrations that are typically more than

10 times those seen in Holocene and Pleistocene varnishes, and this is typical for twentieth-century varnishes because Mn and Fe oxides scavenge lead from anthropogenic sources (Dorn 1998, 2014; Fleisher et al. 1999; Nowinski et al. 2010; Spilde et al. 2013). Note the abrupt textural and chemical boundary between the varnish and the underlying rock (fig. 3), illustrating the accretionary nature of this varnish.

Figure 4 presents budding-bacteria hyphae-like forms similar to those noted previously on the surfaces of rock varnish (Dorn and Oberlander 1981*a*, 1981*b*, 1982; Krumbein and Jens 1981; Krinsley et al. 2009; Wang et al. 2011; Dorn et al. 2012). While many hyphae-like forms occur on varnish surfaces, great enrichment in Mn, Fe, or both is diagnostic of budding bacteria (Aristovskaya and Zavarzin 1971; Aristovskaya and Hirsch 1974; Hirsch 1974; Ghiorse and Hirsch 1979; Ghiorse 1984; Hirsch et al. 1995). For the Erie Canal varnish, EDS analyses on hyphae-like forms show comparative enrichment
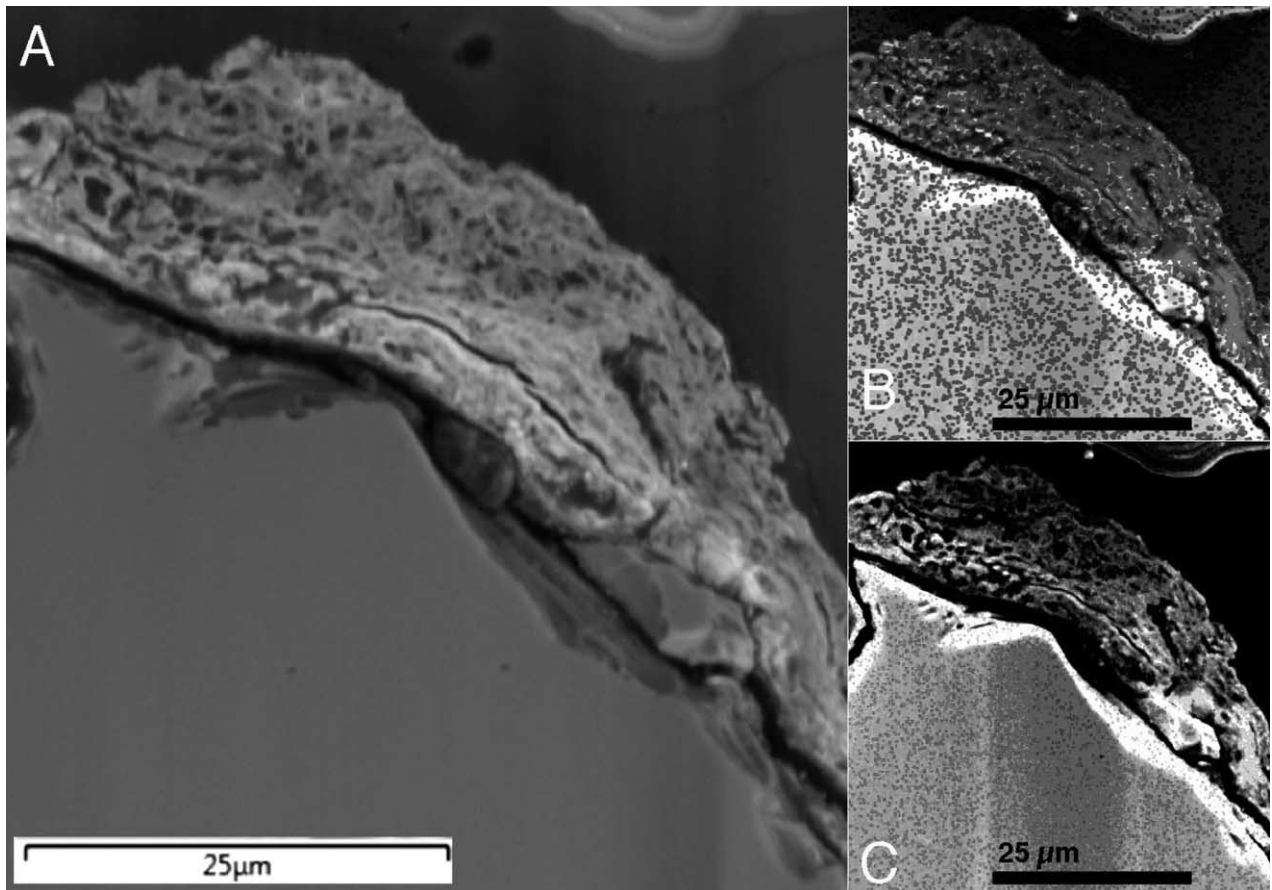

Figure 3. Typical rock varnish accumulating on quartz along the Erie Barge Canal study site, as viewed in cross section with back-scattered electron microscopy (*A*), and energy-dispersive spectroscopy dot maps of Mn (*B*) and Fe (*C*). A color version of this figure is available online.

Table 1. Energy-Dispersive Spectroscopy Semiquantitative Analysis of the Erie Canal Varnish Acquired in a 10-μm Square Placed in the Center of the Varnish Imaged in Figure 4

Element	Line type	Wt%	Wt% 1σ error
C	K series	2.79	.18
O	K series	44.04	.15
Mg	K series	.86	.03
Al	K series	4.09	.04
Si	K series	7.93	.05
P	K series	.74	.05
K	K series	.83	.02
Ca	K series	1.48	.03
Ti	K series	.19	.03
Mn	K series	26.05	.12
Fe	K series	8.21	.09
Zn	L series	1.65	.07
Ba	L series	.95	.08
Pb	M series	.17	.08
Total		100.00	

in Fe (fig. 4*A1*) relative to adjacent varnish (fig. 4*A2*) and also comparative enrichment in Mn (fig. 4*B1*) relative to adjacent varnish (fig. 4*B2*).

Figures 5–7 present the first observations of budding-bacteria hyphae forms that are encrusted in Mn and Fe from within internal layers of varnish. Figure 5 is derived from a depth of ~5 μm beneath the varnish surface, while figure 6 came from a depth of ~8 μm and figure 7 from a depth of ~10 μm. In figures 5 and 6, hyphae forms emerge from cocci forms that are also oxide encrusted. The hyphae forms (figs. 5–7) are considerably smaller than the original hyphae; ongoing diagenesis appears to have remobilized Mn and Fe, and this would facilitate some compression of the form once the bacterium itself died. In all cases, the imaged hyphae forms are not the bacteria but casts of the former hyphae now encrusted in Mn and Fe oxides, where the nanoscale
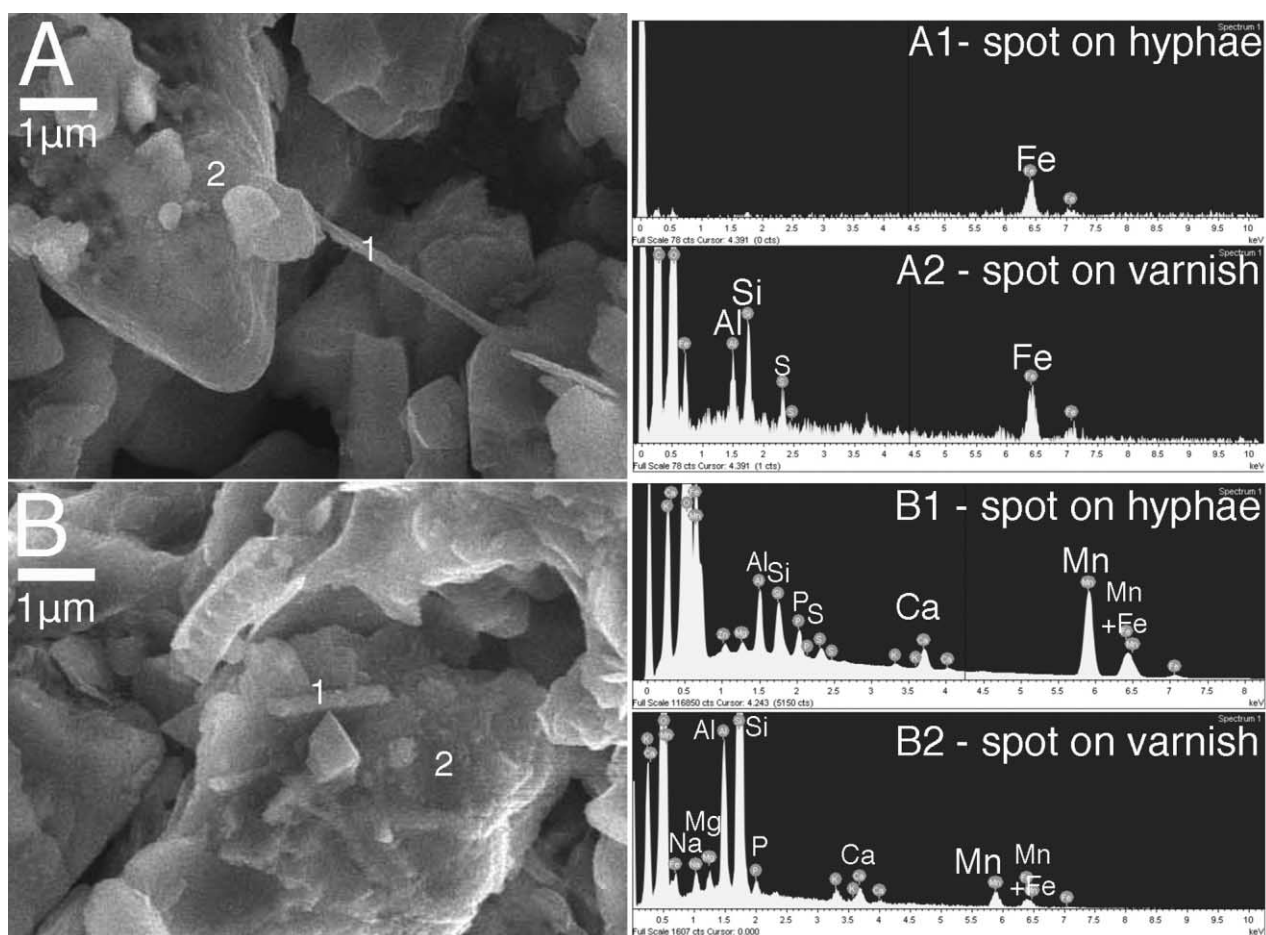
Figure 4. *A*, The surface of Erie Canal varnish, examined with secondary electrons and energy-dispersive spectroscopy (EDS), shows hyphae-like forms encrusted in Fe (point 1) greatly enriched compared to typical EDS spot analyses on adjacent varnish (point 2). *B*, Other hyphae-like forms or fragments of forms reveal a great enrichment in Mn and some Fe (point 1) compared to typical EDS spot analyses of adjacent varnish (point 2).
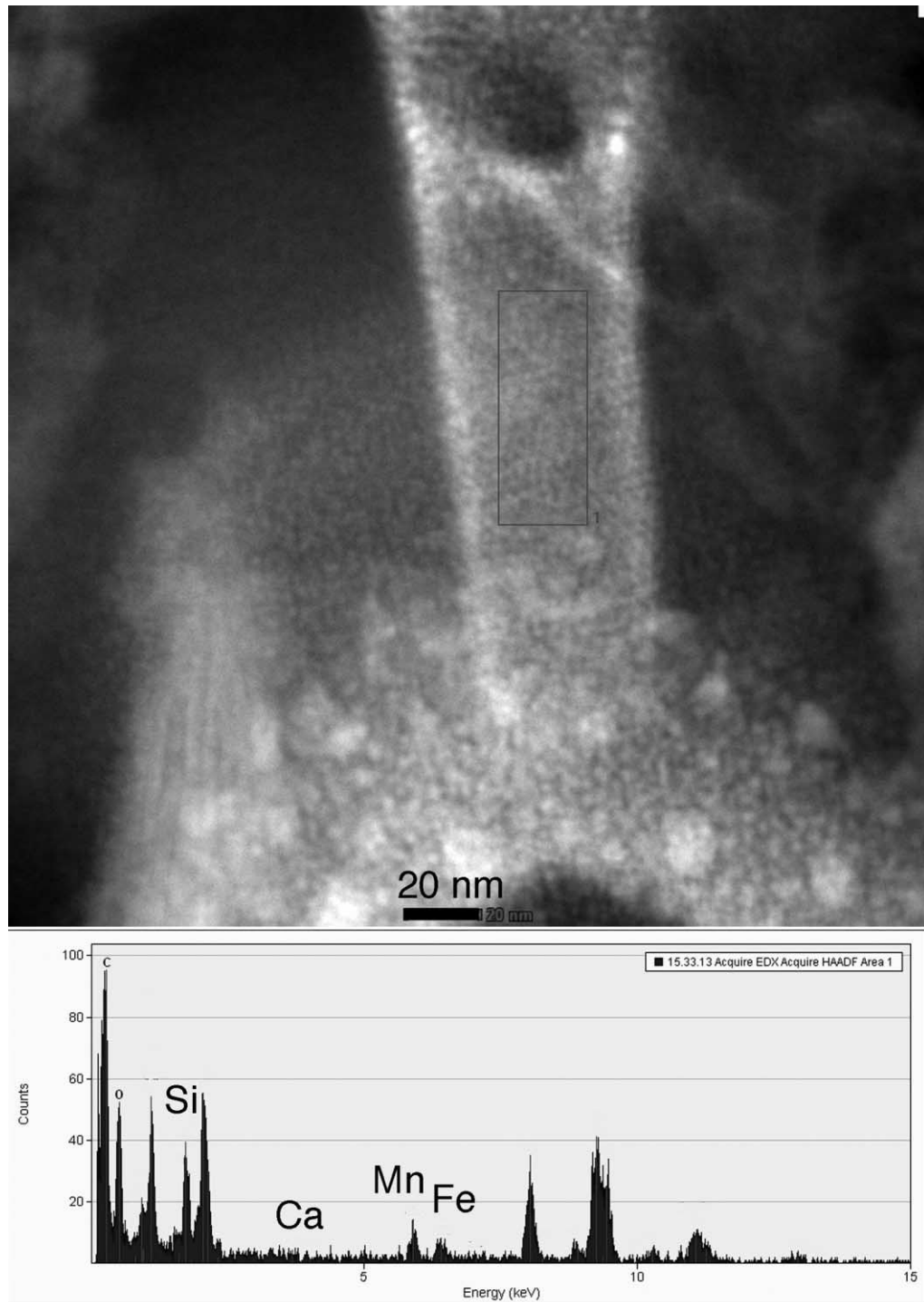
Figure 5. Budding-bacteria hyphae form emerging from a cocci form. The energy-dispersive spectroscopy (EDS) spectrum measured in the box consists mostly of artifacts associated with mounting and preparation of the sample, and thus these artifact peaks are unlabeled. Additional annotation of the EDS spectrum with a larger font identifies the composition of the hyphae form as mostly Mn and Fe, with some Si and Ca.
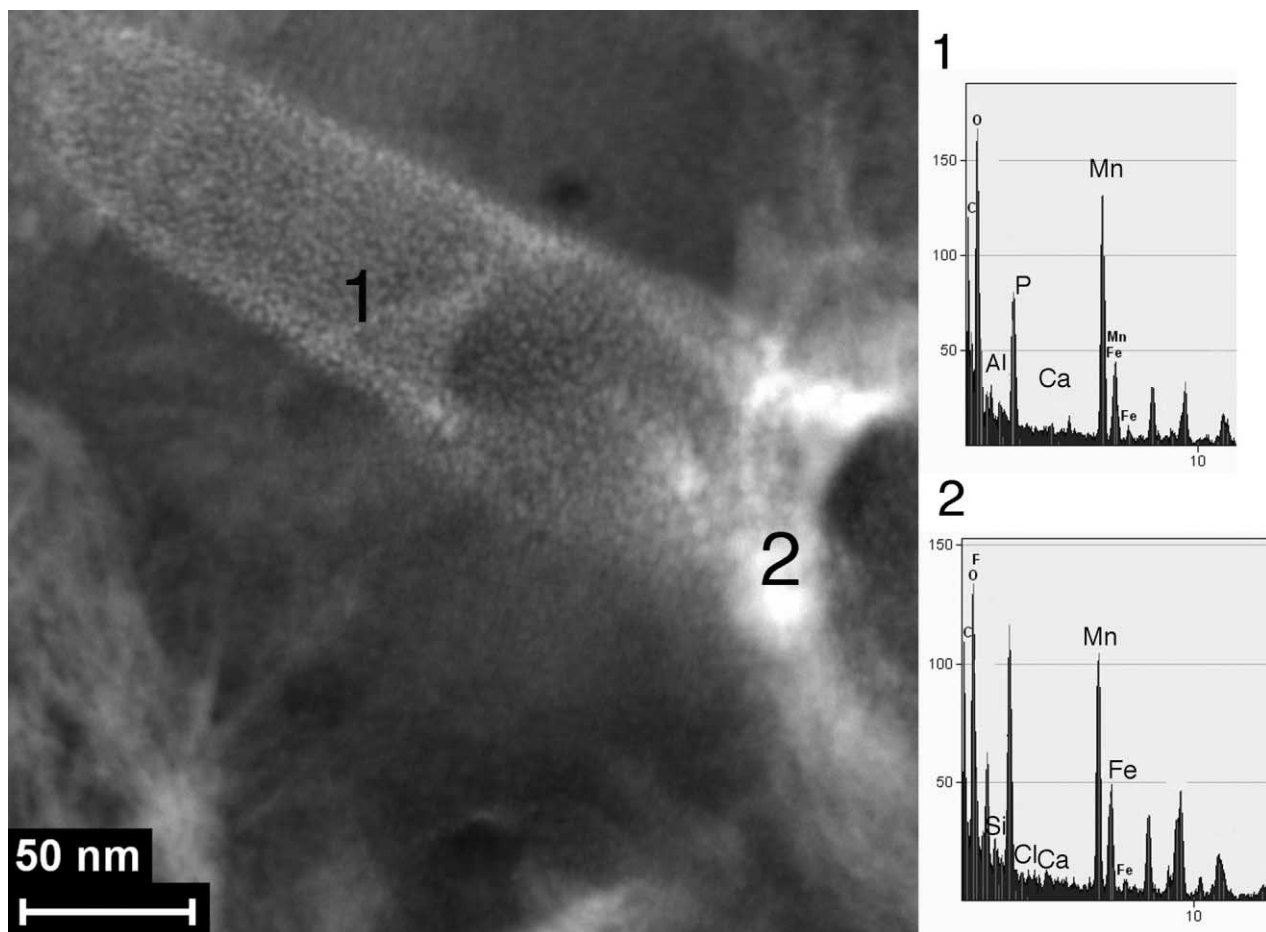
Figure 6. Budding-bacteria hyphae form (point 1) emerging from a cocci form (point 2). The energy-dispersive spectroscopy (EDS) spectra consist mostly of peaks associated with mounting and preparation of the sample, and thus artifacts are not labeled. Larger-font annotation of the EDS spectra identifies the composition of the hyphae form at point 1 as consisting of large Mn and P peaks, with much smaller Fe, Al, and Ca peaks. The spectrum of point 2 contains much less P than those of point 1.

texture of the oxides is granular in figures 5 and 6 and stringy in figure 7.

In addition to budding-bacteria hyphae forms, EDS measured nanoscale chemical variations in a cross section of a cocci bacterial form (fig. 8). Again, this bacterial form is considerably smaller than it would have been as a live bacterium encrusted by oxides, because ongoing remobilization of the oxide cast facilitates compression and shrinkage from an original diameter of likely ~1 μm. The bacterial cast observed in cross section reveals a granular texture where the granules vary in size from <1 to ~10 nm. The elemental chemistry varies from place to place, with EDS spots 1 and 2 being greatly enriched in Mn while EDS spots 3 and 4 are rich in Fe (fig. 8).

While most of the observed Erie Canal varnish does not have a microstromatolitic form (e.g., fig. 3), stromatolite-like textures do exist—as seen in cross

section with BSE microscopy (fig. 9). The sum EDS spectrum for the overall form is quite similar to that for clay-rich varnishes found in warm deserts (Dorn and Oberlander 1982). The nanoscale laminations seen in BSE images do not appear to contain Mn-poor/Mn-rich banding, as revealed by consistent patterns in the Mn and Fe dot maps. The outer few microns contain pores (fig. 9A, 9C) that are partially filled with stringy textures of Mn-rich material (fig. 9B, 9D). These Mn-rich stringy textures could have originated from bacterial precipitates that are now experiencing mobilization of the Mn-Fe precipitated material.

The Mn-rich stringy textures observed in figures 7 and 9 could potentially be the original texture of the Mn-Fe bacteria precipitate. Figure 10 illustrates that stringy textures can also be dominated by Fe (fig. 10A), have similar abundances of Mn and Fe
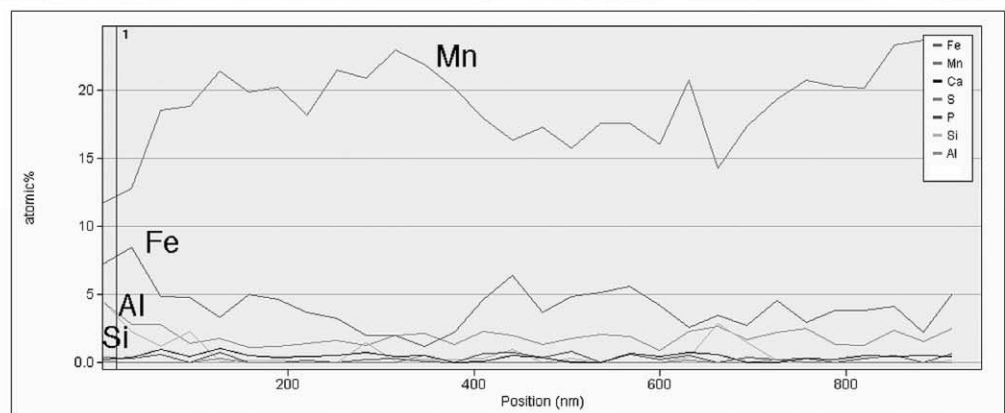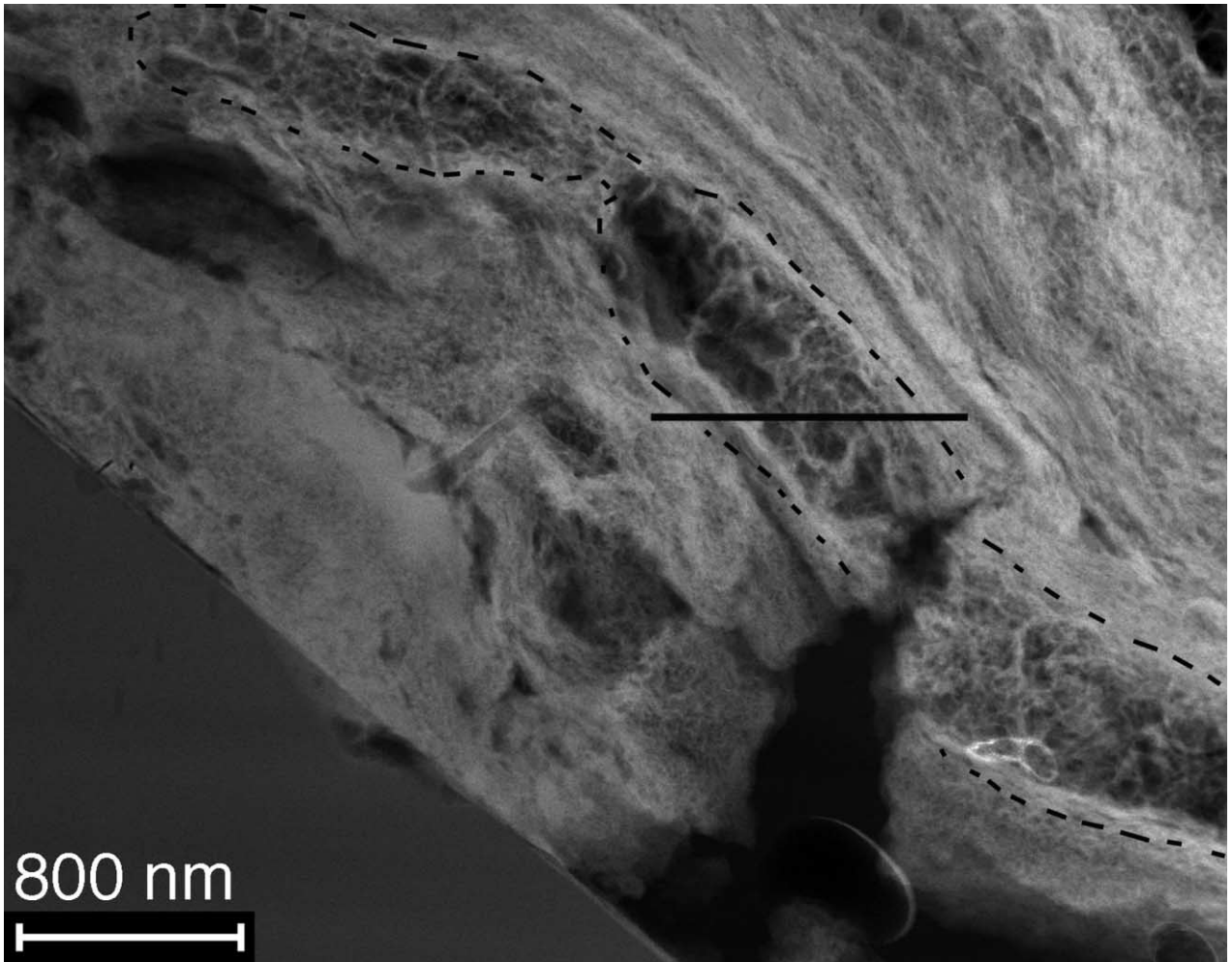
Figure 7. Budding-bacteria hyphae form resting conformably between varnish layers that accreted on the underlying quartz mineral. Dashed lines identify the hyphae form, and the solid line indicates the location of an energy-dispersive spectroscopy transect measuring nanoscale changes in atomic weight percent, dominated by Mn and, to a lesser extent, Fe.
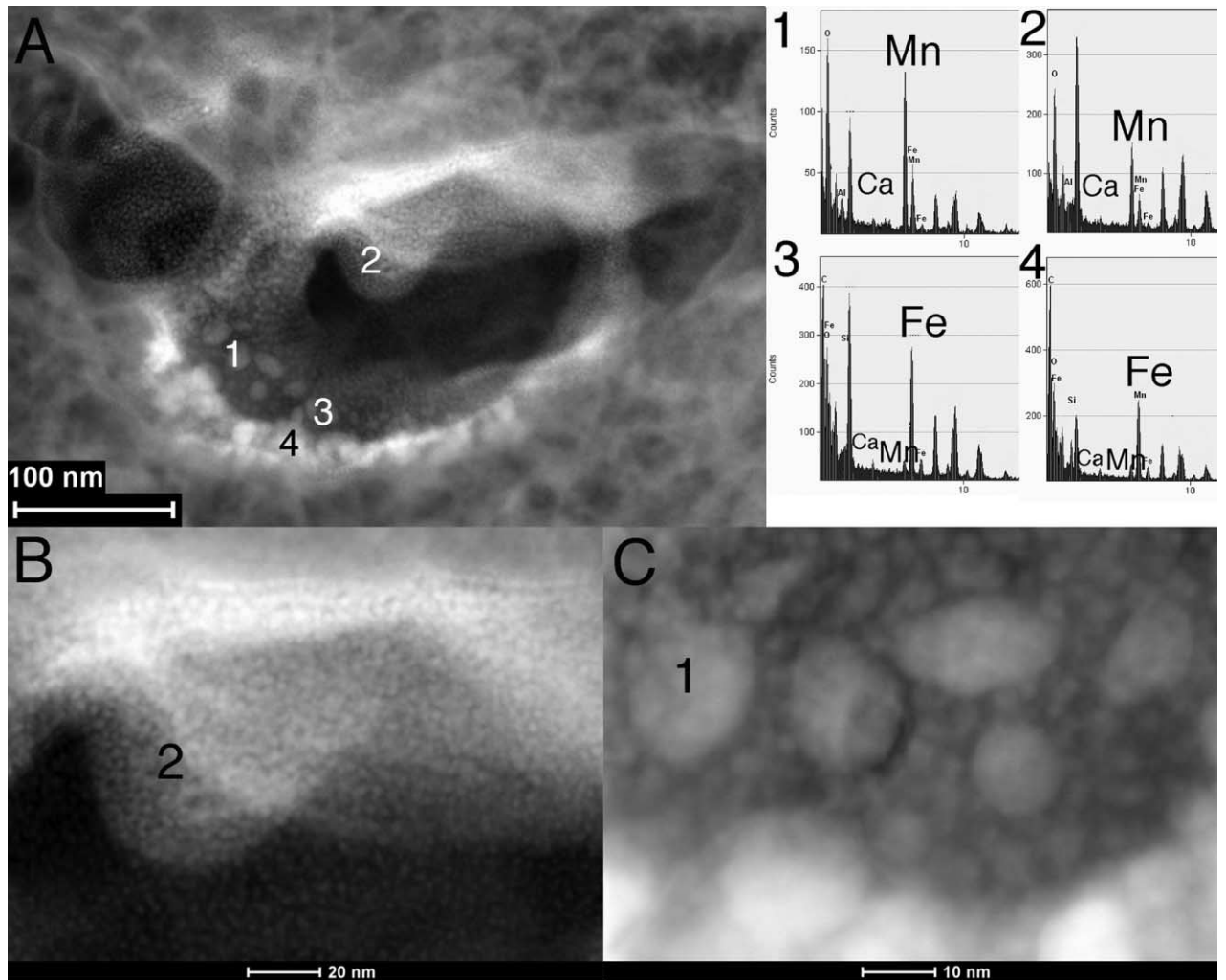
Figure 8. Bacterial cocci form observed in cross section. Points 1–4 in *A* identify the different locations of energy-dispersive spectroscopy (EDS) measurements, and *B* and *C* show close-ups of the granular textures associated with EDS points 2 and 1, respectively. Most of the peaks in these EDS spectra are artifacts associated with sample preparation, and thus these artifact peaks are unlabeled. Major peaks such as Ca, Mn, and Fe are annotated in a larger font. Points 1 and 2 are dominated by Mn, while points 3 and 4 are dominated by Fe.

(fig. 10*B*), or be dominated by Mn (figs. 7, 9, 10*B*). Alternatively, the stringy texture could be a consequence of dissolution of the original bacterial oxide precipitates. After the original precipitated material dissolves, it reprecipitates and alters the texture of the clay minerals, as seen in figure 11.

Discussion

This discussion links our results to four themes in prior scholarship. First, our nanoscale observations of budding-bacteria forms able to precipitate Mn, Fe, or both with granular and stringy textures resonate with observations of similar textures associated with budding bacteria in culturing studies. The

second theme is that our results support the polygenetic model of varnish formation that mixes biotic and chemical processes. The third theme elaborates on prior observations that there are far more potential agents of varnish formation than could be explained by the thickness of varnish deposits—and we discuss the implications of the "varnish rate paradox" in the context of the Erie Canal results. The last aspect of the discussion focuses on implications of these findings for interpreting dark Mn-rich coatings in warm deserts and on Mars.

Erie Canal Results Meet Expectations from Culturing Studies. Cultured budding bacteria are able to concentrate Mn, Fe, or both together (Aristovskaya and Zavarzin 1971; Aristovskaya and Hirsch 1974; Hirsch
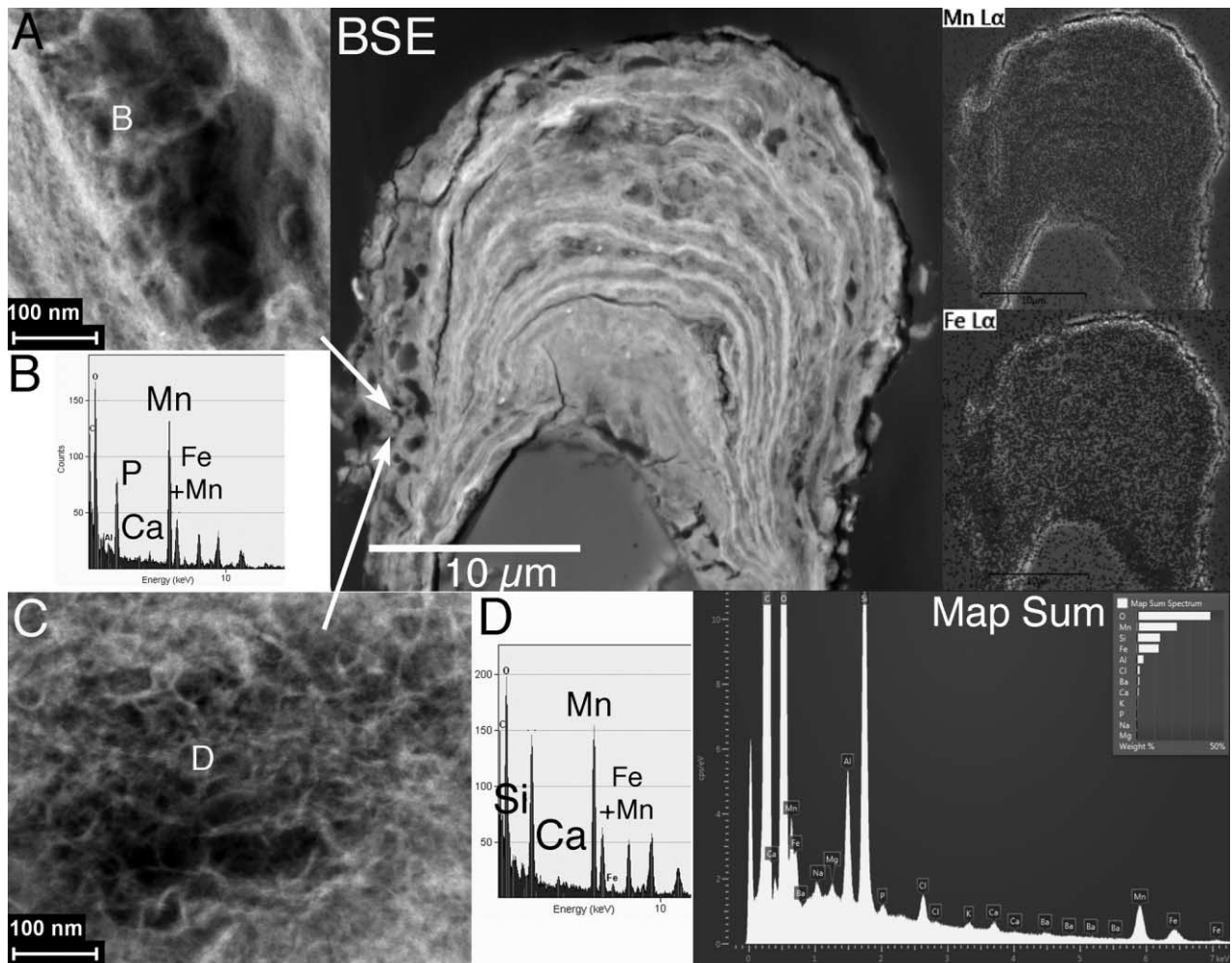
Figure 9. A stromatolitic form observed in back-scattered electron (BSE) microscopy in cross section is dominated by Mn, as revealed by the energy-dispersive spectroscopy (EDS) map sum spectrum. EDS dot maps of Mn and Fe reveal that the observed nanoscale laminae do not favor Mn or Fe. Instead, variations in brightness are caused by clay-rich darker layers. Close-ups of pore spaces in the outer micron of the varnish in *A* and *C* reveal the presence of Mn-rich stringy textures that could be bacterial precipitates undergoing dissolution from the mobilization of the Mn-Fe. A color version of this figure is available online.

1974; Ghiorse and Hirsch 1979; Ghiorse 1984; Hirsch et al. 1995; Braun et al. 2009).

Most bacteria surfaces are charged at neutral pH because of the ionization of the reactive chemical groups which stud them . . . many bacteria can concentrate dilute environmental metals . . . and initiate the development of fine-grained minerals. . . . Eventually biofilms become so mineralized that the shape and form of the constituent bacteria are preserved and embedded. (Beveridge 1997, p. 378)

The specifics of precipitation processes appears to involve electron transfers to extracellular substrates (Hartshorne et al. 2009). The oxides might also be involved in protecting bacteria from ultraviolet

(UV) radiation damage and desiccation (Daly et al. 2010).

In prior observations at the micron scale, EDS spectra revealed enhancements of both Mn and Fe compared to adjacent varnish (Dorn and Oberlander 1981*a*, 1981*b*, 1982; Krumbein and Jens 1981). In contrast, our nanoscale observations reveal areas of Mn-rich precipitates within a few nanometers of Fe-rich precipitates within single cocci forms (fig. 8) and among different types of deposits (fig. 10). These nanoscale observations that budding bacteria precipitate varying amounts of Mn and Fe correspond to observations in the culturing literature of budding bacteria (Aristovskaya and Zavarzin 1971; Aristovskaya and Hirsch 1974; Hirsch 1974; Ghiorse and
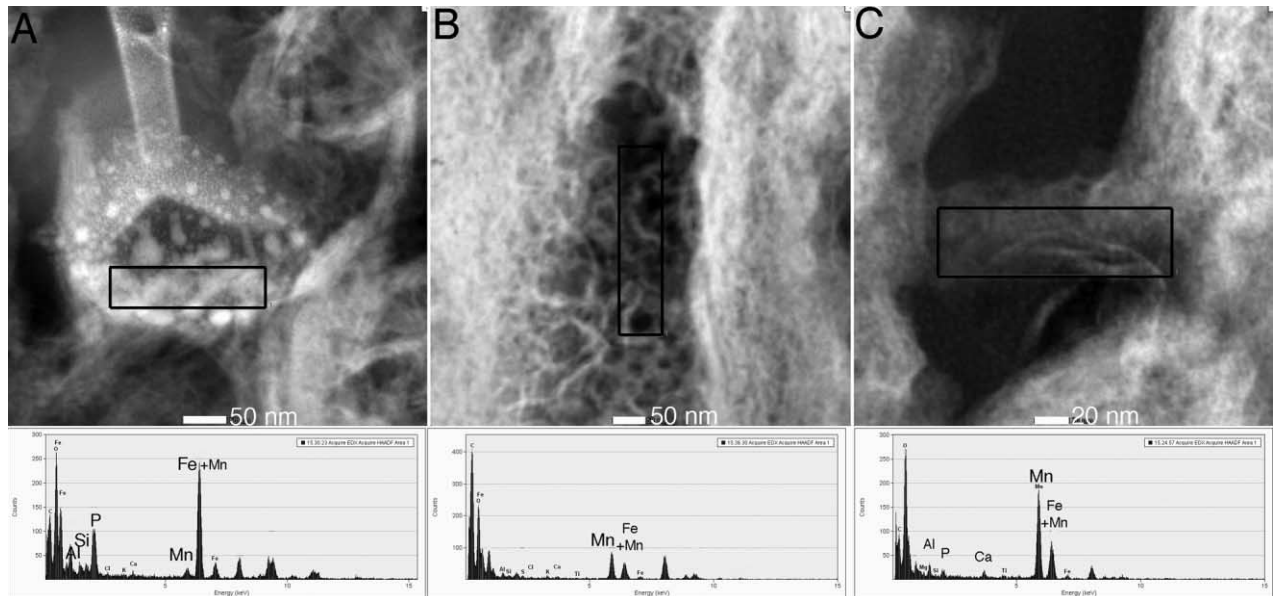
Figure 10.   Stringy textures associated with bacterial forms can have an Fe-rich energy-dispersive spectroscopy (EDS) spectrum (*A*), an EDS spectrum with similar peak sizes for Mn and Fe (*B*), or an Mn-rich EDS spectrum (*C*). The boxes identify the areas measured for the EDS spectra. Most of the peaks in these spectra are artifacts of sample preparation (and are unlabeled), and the major peaks of Al, Si, Ca, Mn, and Fe are labeled with a larger font.

Hirsch 1979; Ghiorse 1984; Hirsch et al. 1995; Braun et al. 2009).

Prior nanoscale observations of bacterial remains in warm desert settings show only granular textures for Mn-Fe encrustations of bacterial cells (Krinsley et al. 1995; Krinsley 1998; Dorn 2007; Dorn et al. 2012, 2013; Larson and Dorn 2012). Granular textures are also observed in the culturing literature on budding bacteria (Aristovskaya and Zavarzin 1971; Aristovskaya and Hirsch 1974; Hirsch 1974; Ghiorse and Hirsch 1979; Ghiorse 1984; Hirsch et al. 1995; Braun et al. 2009).

In addition, the literature associated with bacterial precipitation of Mn and Fe shows the presence of stringy textures (Gebers and Beese 1988; van Waasbergen et al. 1996; Larsen et al. 1999; Villalobos et al. 2003). We observe here for the first time stringy textures that can be Mn rich, Fe rich, or both Mn and Fe enriched (figs. 7, 9, 10). These stringy forms appear similar to birnessite (Mn_2O_4), noted through in situ observations of varnish (Krumbein and Jens 1981) and culturing experiments (Learman et al. 2011). The mobilization and reprecipitation of Mn and Fe at the nanoscale has been recognized widely as a part of the varnishing process (Krinsley et al. 1995, 2009, 2013; Krinsley 1998; Dorn et al. 2012, 2013; Macholdt et al. 2015). We note, therefore, that the stringy textures observed in this study

(figs. 7, 9, 10) could potentially be a product of this ongoing diagenesis.

Erie Canal Results Consistent with Polygenetic Model of Varnish Formation.   The polygenetic model of varnish formation (Dorn 1998, 2007; Krinsley 1998; Krinsley et al. 2013) starts with bacteria concentrating Mn and Fe (figs. 4–10). Then, the Mn-Fe precipitates begin to dissolve, and this facilitates shrinkage and breaks apart the bacterial casts of Mn and Fe. The Mn and Fe then are reprecipitated in association with clay minerals (fig. 11), where birnessite-family minerals dominate manganese in rock vanish (Potter and Rossman 1977, 1978, 1979*a*, 1979*b*, 1979*c*; Potter 1979; McKeown and Post 2001). In this study, bacterial deposits appear to have stringy and granular textures that release nanoscale Mn-Fe to deposit between clay minerals (fig. 11). Potter (1979) argued for this step:

Deposition of the manganese and iron oxides within the clay matrix might then cement the clay layer . . . the hexagonal arrangement of the oxygen in either the tetrahedral or octahedral layers of the clay minerals could form a suitable template for crystallization of the layered structures of birnessite. The average 0–0 distance of the tetrahedral layer is 3.00 Å in illite-montmorillonite mixed-layered clays, which differs only 3.4 percent from the 2.90 Å distance of the hexagonally closed-packed oxygens in birnessite. (p. 174–175)
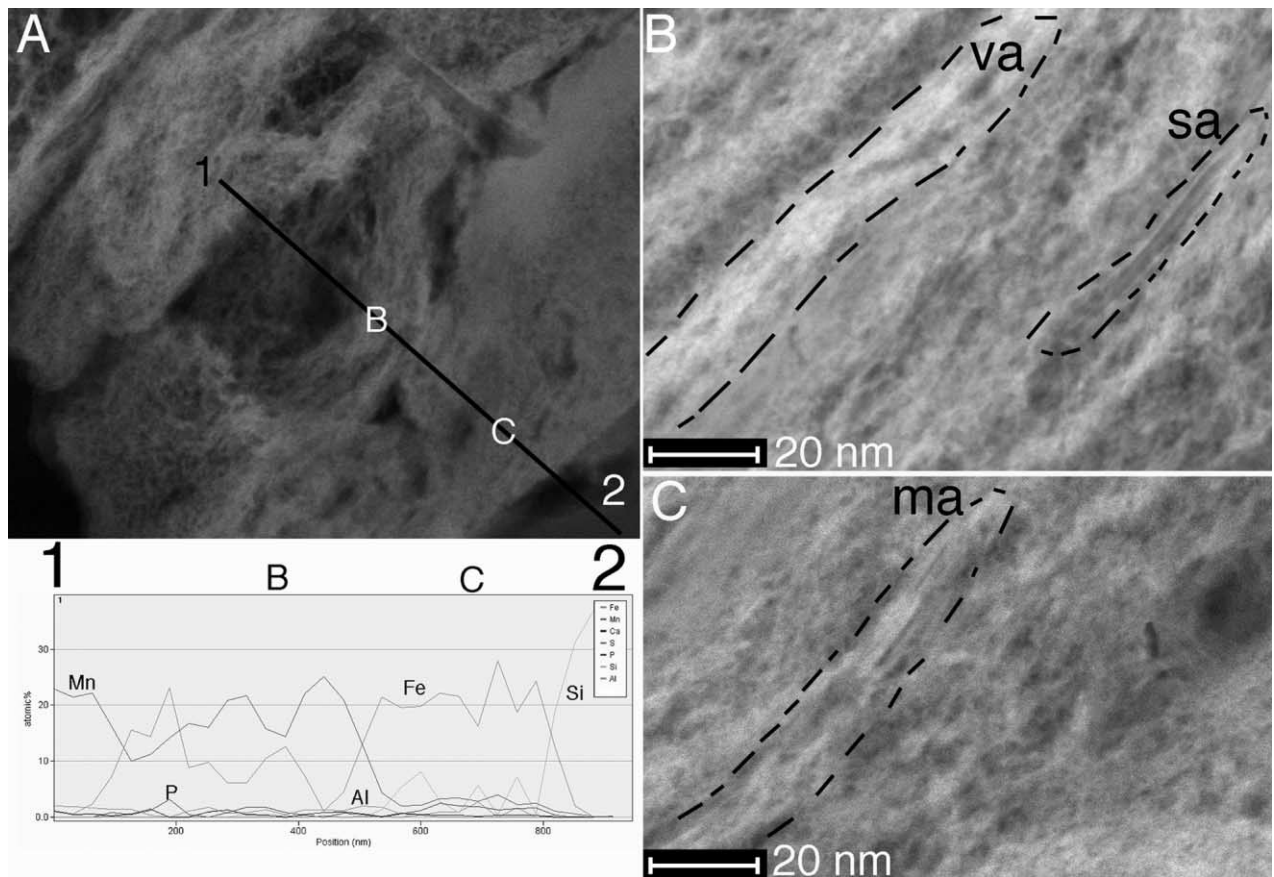
Figure 11. Precipitation of Mn and Fe appears to alter the texture of clay mineral fragments. *A*, 1-μm-long energy-dispersive spectrometry transect from position 1 to position 2 (ending on quartz with a strong Si signature). The transect runs through areas where Mn and Fe trade off as the dominant element in atomic weight percent (other than oxygen, which is not shown). Higher-resolution images *B* and *C* show "pods" of clay mineral structures in different states of alteration through the precipitation of Mn and Fe. *B* identifies very altered (va) and slightly altered (sa) features in the Mn-rich zone, while *C* identifies a moderately altered (ma) feature in the Fe-rich zone.

Potter's explanation for the importance of clay minerals is supported by these findings and other high-resolution nanoscale data (Dorn 1998; Krinsley 1998; Dorn et al. 2012; Krinsley et al. 2013).

McKeown and Post (2001) go on to explain that Mn oxides in varnish undergo transformations even after precipitation in clay minerals:

Even if analysis methods are improved, the situation will remain complicated by the flexibility and great variety of Mn oxide structures. The common elements of these structures enable them to easily intergrow with and transform with one another. Furthermore, many of the phases, particularly the layered structures, readily exchange interlayer cations in response to even slight changes in chemistry on a microscale. (p. 712)

Varnishing thus starts with bacterial encrustation of Mn-Fe but relies on nanoscale mobilization and reprecipitation of the oxides in association with clay minerals. This ongoing diagenesis shifts Mn-Fe at the nanoscale, even though the laminations observed at the micron scale are stable for millennia (Liu and Broecker 2013).

The Varnish Rate Paradox. This portion of the discussion connects the Erie Canal findings to a "varnish rate paradox" identified previously (Dorn 2007; Dorn and Krinsley 2011). An explanation of this paradox starts with the basic observation that typical varnishes formed in warm deserts grow at rates of microns per millennium (Dorn 1998; Liu and Broecker 2000). The most rapidly forming varnishes at the Erie Canal, the Fontana slag deposit (Dorn and Meek 1995), and other locations (Spilde et al. 2013; Dorn 2014) are exceptions.

The second part of the rate paradox rests on the observation that all but one of the proposed mechanisms of varnish formation would generate rates of accretion far greater than those observed in nature:

(1) abiotic processes to enhance Mn in varnish, (2) organisms noted to oxidize Mn and Fe in culturing studies to generate varnish, and (3) organic material extracted in bulk samples (e.g., DNA and other studies) to generate varnish. We analyze each of these three mechanisms in turn to explain why a rate-limiting step does not exist.

1. The idea of varnish formation through abiotic oxidation of Mn has remained unfalsified for the past 6 decades (Engel 1957; Krauskopf 1957; Engel and Sharp 1958) and has remained in the varnish literature (Hooke et al. 1969; Haberland 1975; Whalley 1983; Soleilhavoup 2011). Still, the geomorphic distribution of rock varnish poses at least 11 obstacles (Dorn 1998, p. 242–243) that have yet to be analyzed by proponents of the abiotic hypothesis. Each year, carbonic acid in rainfall falls on dust that has accumulated on varnished surfaces in warm deserts, and the abiotic hypothesis requires that this weak acid leach Mn out of the dust, followed by reprecipitation through slight increases in pH as water evaporates. Dorn (2007, p. 265) calculated that known rates of dust deposition in a typical warm desert setting and concentrations of Mn in this dust would generate varnishes 100–10,000 times faster than empirical rates of varnishing on the order of microns per millennium (Dorn 1998; Liu and Broecker 2000). More recent variations on this abiotic hypothesis (Madden and Hochella 2005; Goldsmith et al. 2014) similarly do not contain a rate-limiting step. Thus, if abiotic processes generate varnish, rates would be several orders of magnitude more rapid than empirical observations.

2. Culturing studies of genera oxidizing Mn and Fe in varnish note a great number of different organisms (Krumbein 1969; Dorn and Oberlander 1981a; Krumbein and Jens 1981; Billy and Blanc 1982; Staley et al. 1983, 1991; Taylor-George et al. 1983; Palmer et al. 1985; Hungate et al. 1987; Adams et al. 1992; Grote and Krumbein 1992; Eppard et al. 1996; Sterflinger et al. 1999; Perry et al. 2004a, 2004b; Northup et al. 2010). If all of these organisms assist in the formation of varnish, rates should be as fast as those of other nonvarnish Mn-Fe deposits (Francis 1921; Ferris et al. 1987; Konhauser et al. 1994; Kennedy et al. 2003)—several orders of magnitude faster than empirical observations of warm desert varnishes.

3. Different sorts of studies have analyzed "bulk" samples requiring the scraping of varnish (and underlying weathering rind and rock material). These studies have reported on the presence of a variety of types of organic material, including amino acids (Warsheid 1990; Nagy et al. 1991; Perry et al. 2003; Perry and Kolb 2003), isotopes of carbon (Dorn and DeNiro 1985), fatty acid methyl esters (Schelble et al. 2005), and genetic material providing phylogenetic insight (Eppard et al. 1996; Perry et al. 2004a; Kuhlman et al. 2005, 2006a, 2006b, 2008; Benzerara et al. 2006; Northup et al. 2010; Esposito et al. 2015). All of these analyses reveal that a wide variety of organisms exist on, within, and under rock varnishes, and if only a small fraction of these were involved in varnishing, rates would be much faster than empirically observed.

The solution to the paradox, that varnish typically forms slowly despite the lack of a rate-limiting step in proposed mechanisms of Mn enhancement, must rest in a severe rate-limiting step associated with Mn and Fe enhancement. At the present time, scholarship on rock (or desert) varnish offers only one piece of empirical insight into this issue: the rarity of direct in situ observations of bacteria enhancing Mn and Fe on varnish surfaces (fig. 5; Taylor-George et al. 1983; Jones 1991; Dorn et al. 1992; Dorn 1998; Krinsley et al. 2009, 2012; Wang et al. 2011). Even less frequent are in situ observations of bacterial forms encrusted in Mn and Fe within varnish microstratigraphies (Dorn and Meek 1995; Dorn 1998; Krinsley 1998; Flood et al. 2003; Allen et al. 2004; Krinsley et al. 2009, 2013).

These rare in situ observations are sufficient to explain the slow rates of varnishing observed in deserts (Dorn and Krinsley 2011). The following assumptions allow an estimate of how many bacterial cells encrusted in oxides would be required to generate varnishes found in warm deserts: (1) one bacterial cast composed of Mn-Fe oxides consists of a thickness of ~100 nm of oxides on both sides of a cell (Dorn 1998, p. 244–245); (2) a typical varnish formed in warm deserts consists of 70% clay minerals (Potter and Rossman 1977); and (3) a reasonably typical thickness of warm desert varnishes that are ~10,000 y old would be ~20 μm (Liu and Broecker 2000, 2008; Dorn 2012). By redistributing the 100 nm of oxides into clay minerals, one bacterium would be responsible for ~800 nm of varnish material. To then generate 20 μm would require only about 25 oxide-encrusted cells, or 1 oxide-encrusted bacterial cell in about 400 y. If we vary these assumptions and consider different rates of ongoing diagenesis that removes Mn-Fe from varnish and redeposits it in the underlying weathering rind (Gordon and Dorn 2005; Dorn et al. 2013), the number of oxide-encrusted cells required to produce varnish could vary by an order of magnitude in either direction. However, the conclusion remains clear: only a few bacteria every century to millennium would be needed to generate typical observed rates of varnishing in warm deserts.

If the extremely rare occurrence of oxide-encrusted bacteria is the rate-limiting step needed to explain the "varnish rate paradox," then the Erie Canal var-

nishing site showing very rapid rates of varnishing poses an interesting assessment of the paradox. The nanoscale imagery of this study reveals a much more accurate portrayal of the thickness of the oxide cast associated with budding-bacteria hyphae or cocci; thicknesses range between 20 and 400 nm. In the Erie Canal varnishes, oxides are much more abundant than in typical warm desert settings, with typical ratios of oxides to clays of about 1:1. With a thickness of 50 nm for a bacterial cast, 1 bacterium would potentially generate ~100 nm of varnish. With a varnish thickness of ~15 μm, 150 bacteria+clays would be required to generate the raw varnish material. With an age of 100 y, it would only take 1–2 bacteria growing each year to generate the observed Erie Canal varnishing. With thicker encrustations or with a greater abundance of clays, even fewer bacteria would be required.

If each bacterium lived and processed Mn and Fe for 10 d, the chances of "catching a bacterium in the act" at the Erie Canal (e.g., fig. 4) would be highly unlikely, at somewhere around 2%–3%. Similarly, if each bacterium responsible for varnishes found in warm deserts lived and processed Mn and Fe for 10 d, the chances of actually observing the Mn-Fe enhancement would 10 d out of ~400 y, or somewhere on the order of 1 d in 15,000.

Mn-Rich Rock Varnish in Warm Deserts and on Mars. The rarity of fossil casts of Mn-rich bacteria in warm deserts (Dorn 1998, 2009; Dorn and Krinsley 2011), with the exception of anomalously fast-growing varnishes (Dorn and Meek 1995), could be explained most simply by the high UV exposure, heat, and xeric conditions experienced by exposed rock surfaces (Dorn and Oberlander 1982; Viles 1995). In this hypothesis, microenvironments with greater moisture foster the growth of competing lithobionts, such as microcolonial fungi and lichens (Dragovich 1987; Dorn 2010). The observed rock varnish on the south-facing north side of the Erie Canal exists at an angle of about 45°; thus, our hypothesis is that this microenvironmental setting provides the maximum possible UV and solar radiation exposure and allows the rock surfaces to dry out sufficiently to reduce lithobiont competition to the budding bacteria.

The number one National Aeronautics and Space Administration (NASA) goal for Mars exploration rests in determining whether Mars ever supported life (MEPAG 2015). Accordingly, important subgoals include determining "if localities having high combined potential for modern habitability and biosignature presence host evidence for extant life" and in testing "for the presence of possibly biogenic physical structures, from microscopic (micron-scale)

to macroscopic (meter-scale), combining morphological, mineralogical, and chemical information where possible" (MEPAG 2015, p. 11).

The question of rock varnish on Mars has persisted since NASA's Viking Lander program (Guinness et al. 1996), when its cameras spotted shiny, dark rock coatings. Other NASA missions also reported similar sitings associated with Mars Pathfinder in 1997 (Kraft and Greeley 2000) and the twin Mars Exploration Rovers in 2007 (Arvidson et al. 2014). Confirmation of thin, dark coatings rich in Mn on the surface of rocks in Gale Crater on Mars occurred in 2012 via NASA's Mars Science Laboratory Curiosity (Lanza et al. 2014). The connection between Mars's rock varnish and the search for life (DiGregorio 2002) would likely follow a similar path as that on Earth—evaluating abiotic and biotic mechanisms for Mn enhancement.

While abiotic processes could concentrate Mn on Mars (Ming et al. 2015), this and prior research (Krumbein and Jens 1981; Grote and Krumbein 1992; Krinsley 1998; Krinsley and Rusk 2000; Krinsley et al. 2009, 2012) emphasizes the importance of microstratigraphic analyses at the micron scale and nanoscale for determining whether biotic processes are involved in terrestrial Mn-rich rock varnish formation. Thus, future discussions on the significance of Mn-rich rock coatings and the search for life on Mars might require similar nanoscale microstratigraphic insight.

Conclusion

Sandstone blocks quarried and placed along the Erie Canal of upper New York State in ~1918 developed rock varnishes with a typical thickness of ~15 μm. In contrast to typical warm desert varnish with a ratio of clays to Mn-Fe oxides of 2:1, this ratio is about 1:1 in Erie Canal varnish. The greater abundance of Mn-Fe is due to a greater abundance of microbial fossils of budding bacteria. Nanoscale imagery and EDS analyses of Mn-Fe encrustations around cocci cells and budding forms reveal that these casts can have granular or stringy textures. Similar to findings of culturing studies of budding bacteria, some of the cellular encrustations are composed only of mostly Mn, some are enriched only in Fe, and some are enriched in both Mn and Fe. After Mn-Fe is mobilized from these budding-bacteria casts, the Mn-Fe is deposited a few nanometers away in a matrix of clay minerals.

Four general explanations exist to explain the Mn-Fe enrichment in rock (or desert) varnish: (1) a polygenetic model, where the rare occurrence of budding bacteria enhances enough Mn and Fe to

remobilize into clay minerals, cementing the clay-oxide matrix to rock surfaces; (2) abiotic processes that enhance Mn to sufficient levels to generate varnish; (3) a host of different Mn-Fe bacteria and fungi cultured from varnish all combine to contribute to varnishing; (4) a wide variety of different bacteria and organic matter that might be involved in varnish formation, as suggested by studies of bulk organic matter and phylogenetic studies of varnish material. Of these explanations, only the polygenetic model has a rate-limiting step that explains the very slow rate of varnishing of microns per millennium observed in warm deserts.

This study provides support for the polygenetic model by studying a site where varnishing rates are 2 orders of magnitude greater than those in warm deserts. Considering vertical rates of accretion, only 150 Mn-Fe-encrusted budding-bacteria cells would be required to provide the ~15-μm-thick Erie Canal varnish. This would take only 1–2 bacteria growing each year. In contrast, one budding-bacterium cast every 400 y would be needed to explain a ~20-μm-thick, 10,000-y-old warm desert varnish.

REFERENCES CITED

Adams, J. B.; Palmer, F.; and Staley, J. T. 1992. Rock weathering in deserts: mobilization and concentration of ferric iron by microorganisms. Geomicrobiol. J. 10:99–114.

Allen, C.; Probst, L. W.; Flood, B. E.; Longazo, T. G.; Schelble, R. T.; and Westall, F. 2004. Meridiani Planum hematite deposit and the search for evidence of life on Mars—iron mineralization of microorganisms in rock varnish. Icarus 171:20–30.

Aristovskaya, T. V. 1961. Accumulation of iron in breakdown of organomineral humus complexes by microorganisms. Dokl. Akad. Nauk SSSR 136:954–957.

———. 1963. Natural forms of existence of soil bacteria. Mikrobiologiya 32:564–658.

Aristovskaya, T. V., and Hirsch, P. 1974. Genus *Pedomicrobium* Aristovskaya 1961. *In* Buchanan, R. E., and Gibbons, N. E., eds. Bergey's manual of determinative bacteriology (8th ed.). Baltimore, Williams & Wilkins, p. 151–153.

Aristovskaya, T. V., and Zavarzin, G. A. 1971. Soil biochemistry. *In* McLaren, A. D., and Skujinš, J., eds. Soil biochemistry. Vol. 2. New York, Dekker, p. 385–408.

Arvidson, R. E.; Catalano, J. G.; Clark, B. C.; Fischer, W. W.; Grotzinger, J. P.; Gellert, R.; Guinness, E. A.; et al. 2014. Manganese in Endeavour Crater rim materials, Mars, and implications for habitability [abs.]: Am. Geol. Union Fall Meeting, San Francisco, December 15–19. Abstract P34A-08. http://abstractsearch.agu.org/meetings/2014/FM/P34A-08.html.

Basedow, H. 1914. Aboriginal rock carvings of great antiquity in South Australia. J. R. Anthropol. Inst. 44:195–211.

Benzerara, K.; Chapon, V.; Moreira, D.; Lopez-Garcia, P.; Guyot, F.; and Heulin, T. 2006. Microbial diversity on the Tatahouine meteorite. Meteorit. Planet. Sci. 41:1259–1265.

Beveridge, T. J. 1997. Ability of bacteria to promote the formation of fine-grained minerals on their surfaces. *In* Hoover, R. B., ed. Instruments, methods, and missions for the investigation of extraterrestrial microorganisms. Proc. SPIE 3111:378–387. doi:10.1117/12.278792.

Billy, C., and Blanc, P. 1982. Synthèse de carbonate et oxyde de manganèse par voie bactérienne. C. R. Acad. Sci. 295:303–305.

Braun, B.; Richert, I.; and Sewzyk, U. 2009. Detection of iron-depositing *Pedomicrobium* species in native biofilms from the Odertal National Park by a new, specific FISH probe. J. Microbiol. Methods 79:37–43.

Brett, C. E.; Tepper, D. H.; Goodman, W. M.; LoDuca, S. T.; and Eckert, B. 1995. Revised stratigraphy and correlations of the Niagaran Provincial Series (Medina, Clinton, and Lockport Groups) in the type area of western New York. U. S. Geol. Surv. Bull. 2086:1–66.

Daly, M. J.; Gaidamakova, E. K.; Matrosova, V. Y.; Kiang, J. G.; Fukumoto, R.; Lee, D-Y.; Wehr, N. B.; Viteri, G. A.; Berlett, B. S.; and Levine, R. L. 2010. Small-molecule antioxidant proteome-shields in *Deinococcus radiodurans*. PLoS ONE 5:e12570. doi:10.1371/journal.pone.0012570.

de Vries, J. L., and Vrebos, B. A. R.. 2002. Quantification of infinitely thick specimens by XRF analysis. *In* van Grieken, R. E., and Markowitz, A. A., eds. Handbook of X-ray spectrometry (2nd ed.). New York, Dekker, p. 341–406.

Diaz, T. A.; Bailley, T. L.; and Orndorff, R. L. 2002. SEM analysis of vertical and lateral variations in desert varnish chemistry from the Lahontan Mountains, Nevada [abs.]: Geol. Soc. Am. Abstr. Program. https://gsa.confex.com/gsa/2002RM/finalprogram/abstract_33974.htm.

DiGregorio, B. E. 2002. Rock varnish as a habitat for extant life on Mars. *In* Hoover, R. B.; Levin, G. V.; Paepe, R. R.; and Rozanov, A. Y., eds. Instruments, methods, and missions for astrobiology IV. Proc. SPIE 4495:120–130. doi:10.1117/12.454750.

Ditto, J.; Krinsley, D.; and Langworthy, K. 2012. Localized grounding, excavation, and dissection using *in-situ* probe techniques for focused ion beam and scanning electron microscopy: experiments with rock varnish. Scanning 34:279–283.

Dorn, R. I. 1998. Rock coatings. Amsterdam, Elsevier.

———. 2007. Rock varnish. *In* Nash, D. J., and McLaren, S. J., eds. Geochemical sediments and landscapes. London, Blackwell, p. 246–297.

———. 2009. Desert rock coatings. *In* Parsons, A. J., and Abrahams, A., eds. Geomorphology of desert environments. Amsterdam, Springer, p. 153–186.

———. 2010. Debris flows from small catchments of the Ma Ha Tuak Range, metropolitan Phoenix, Arizona. Geomorphology 120:339–352.

———. 2012. Do debris flows pose a hazard to mountain-front property in metropolitan Phoenix, Arizona? Prof. Geogr. 64:197–210.

———. 2014. Chronology of rock falls and slides in a desert mountain range: case study from the Sonoran Desert in south-central Arizona. Geomorphology 223: 81–89.

Dorn, R. I., and DeNiro, M. J. 1985. Stable carbon isotope ratios of rock varnish organic matter: a new paleoenvironmental indicator. Science 227:1472–1474.

Dorn, R. I.; Gordon, S. J.; Krinsley, D.; and Langworthy, K. 2013. Nanoscale: mineral weathering boundary. *In* Pope, G. A., ed. Treatise on geomorphology. Vol. 4. San Diego, Academic Press, p. 44–69.

Dorn, R. I., and Krinsley, D. H. 2011. Spatial, temporal and geographic considerations of the problem of rock varnish diagenesis. Geomorphology 130:91–99.

Dorn, R. I.; Krinsley, D. H.; and Ditto, J. 2012. Revisiting Alexander von Humboldt's initiation of rock coating research. J. Geol. 120:1–14.

Dorn, R. I.; Krinsley, D. H.; Liu, T.; Anderson, S.; Clark, J.; Cahill, T. A.; and Gill, T. E. 1992. Manganese-rich rock varnish does occur in Antarctica. Chem. Geol. 99:289–298.

Dorn, R. I., and Meek, N. 1995. Rapid formation of rock varnish and other rock coatings on slag deposits near Fontana. Earth Surf. Processes Landf. 20:547–560.

Dorn, R. I., and Oberlander, T. M. 1981*a*. Microbial origin of desert varnish. Science 213:1245–1247.

———. 1981*b*. Rock varnish origin, characteristics and usage. Z. Geomorphol. 25:420–436.

———. 1982. Rock varnish. Prog. Phys. Geogr. 6:317–367.

Dragovich, D. 1987. Weathering of desert varnish by lichens. *In* Conacher, A., ed. Readings in Australian geography: proceedings of the 21st Institute of Australian Geographers Conference. Perth, Institute of Australian Geographers (WA Branch), p. 407–412.

Duke, W. L. 1991. The lower Silurian Medina Group in New York and Ontario, pt. 4, trip B4. *In* Cheel, R. J., ed. Sedimentology and depositional environments of Silurian strata of the Niagara Escarpment, Ontario and New York: Geological Association of Canada field trip guidebook. Toronto, Geological Association of Canada, p. 35–61.

Engel, C. G. 1957. Desert varnish. MSc thesis, University of California, Los Angeles.

Engel, C. G., and Sharp, R. S. 1958. Chemical data on desert varnish. Geol. Soc. Am. Bull. 69:487–518.

Eppard, M.; Krumbein, W. E.; Koch, C.; Rhiel, E.; Staley, J. T.; and Stackebrandt, E. 1996. Morphological, physiological, and molecular characterization of actinomycetes isolated from dry soil, rocks, and monument surfaces. Arch. Microbiol. 166:12–22.

Esposito, A.; Ahmed, E.; Cizzazzo, S.; Skorski, J.; Overmann, J.; Holmstrom, S. J. M.; and Brusetti, L. 2015. Comparison of rock varnish bacterial communities with surrounding non-varnished rock surfaces: taxon-specific analysis and morphological description. Microb. Ecol. 70:741–750.

Ferris, F. G.; Fyfe, W. S.; and Beveridge, T. J. 1987. Manganese oxide deposition in a hot spring microbial mat. Geomicrobiol. J. 5:33–42.

Fleisher, M.; Liu, T.; Broecker, W.; and Moore, W. 1999. A clue regarding the origin of rock varnish. Geophys. Res. Lett. 26(1):103–106.

Flood, B. E.; Allen, C.; and Longazo, T. 2003. Microbial fossils detected in desert varnish [abs.]: Recognizing and interpreting biosignatures. Abstract 12652. Astrobiology 2(4):608.

Francis, W. D. 1921. The origin of black coatings of iron and manganese oxides on rocks. Proc. R. Soc. Qld. 32: 110–116.

Gebers, R., and Beese, M. 1988. *Pedomicrobium americanum* sp. nov. and *Pedomicrobium australicum* sp. nov. from aquatic habitats, *Pedomicrobium* gen. emend. and *Pedomicrobium ferrugineum* sp. emend. Int. J. Syst. Bacteriol. 38:303–315.

Ghiorse, W. C. 1984. Biology of iron- and manganese-depositing bacteria. Annu. Rev. Microbiol. 38:515–550.

Ghiorse, W. C., and Hirsch, P. 1979. An ultrastructural study of iron and manganese deposition associated with extracellular polymers of *Pedomicrobium*-like budding bacteria. Arch. Mikrobiol. 123:213–226.

Goldsmith, Y.; Stein, M.; and Enzel, Y. 2014. From dust to varnish: geochemical constraints on rock varnish formation in the Negev Desert, Israel. Geochim. Cosmochim. Acta 126:97–111.

Gordon, S. J., and Dorn, R. I. 2005. In situ weathering rind erosion. Geomorphology 67:97–113.

Grote, G., and Krumbein, W. E. 1992. Microbial precipitation of manganese by bacteria and fungi from desert rock and rock varnish. Geomicrobiology 10: 49–57.

Guinness, E. A.; Arvidson, R. E.; and Shepard, M. K. 1996. Specular scattering from rock surfaces at the Viking Lander sites. *In* 27th Lunar and Planetary Science Conference, p. 471–472. http://www.lpi.usra.edu/meetings /lpsc1996/pdf/1236.pdf.

Haberland, W. 1975. Untersuchungen an Krusten, Wustenlacken und Polituren auf Gesteinsoberflachen der nordlichen und mittleren Saharan (Libyen und Tchad). Berl. Geogr. Abh. 21:1–77.

Hartshorne, R. S.; Reardon, C. L.; Ross, D.; Nuester, J.; Clarke, T. A.; Gates, A. J.; Mills, P. C.; et al. 2009. Characterization of an electron conduit between bacteria and the extracellular environment. Proc. Natl. Acad. Sci. USA 106:22169–22174.

Hirsch, P. 1974. The budding bacteria. Annu. Rev. Microbiol. 28:391–444.

Hirsch, P., and Conti, S. F. 1964. Biology of budding bacteria. II. Growth and nutrition of *Hyphomicrobium* spp. Arch. Mikrobiol. 48:358–367.

Hirsch, P.; Eckhardt, F. E. W.; and Palmer, R. J., Jr. 1995. Methods for the study of rock-inhabiting microorganisms—a mini review. J. Microbiol. Methods 23:143–167.

Hooke, R. LeB.; Yang, H.; and Weiblen, P. W. 1969. Desert varnish: an electron probe study. J. Geol. 77:275–288.

Hungate, B.; Danin, A.; Pellerin, N. B.; Stemmler, J.; Kjellander, P.; Adams, J. B.; and Staley, J. T. 1987. Characterization of manganese-oxidizing (MnII→MnIV) bacteria from Negev Desert rock varnish: implications in desert varnish formation. Can. J. Microbiol. 33:939–943.

Israel, E. J.; Arvidson, R. E.; Wang, A.; Pasteris, J. D.; and Jolliff, B. L. 1997. Laser Raman spectroscopy of varnished basalt and implications for in situ measurements of Martian rocks. J. Geophys. Res. 102(E12):28705–28716.

Ivanova, N.; Sikorski, J.; Jando, M.; Munk, C.; Lapidus, A.; del Rio, T. G.; Copeland, A.; et al. 2010. Complete genome sequence of *Geodermatophilus obscurus* type strain (G-20T). Stand. Genomic Sci. 2:158–167.

Jones, C. E. 1991. Characteristics and origin of rock varnish from the hyperarid coastal deserts of northern Peru. Quat. Res. 35:116–129.

Keim, C. N.; Nalini, H. A.; and de Lena, J. C. 2015. Manganese oxide biominerals from freshwater environments in Quadrilatero Ferrifero, Minas Gerais, Brazil. Geomicrobiol. J. 32:549–559.

Kennedy, C. B.; Scott, S. D.; and Ferris, F. G. 2003. Characterization of bacteriogenic iron oxide deposits from Axial Volcano, Juan de Fuca Ridge, northeast Pacific Ocean. Geomicrobiol. J. 20:199–214.

Khak-mun, T. 1966. Iron- and manganese-oxidizing microorganisms in soils of South Sakhalin. Microbiology 36 (2):276–281.

———. 1968. The biological nature of iron-manganese crusts of soil-forming rocks in Sakhalin mountain soils. Mikrobiologiya 37:749–753.

Konhauser, K. O.; Fyfe, W. S.; Schultze-Lam, S.; Ferris, F. G.; and Beveridge, T. J. 1994. Iron phosphate precipitation by epilithic microbial biofilms in Arctic Canada. Can. J. Earth Sci. 31:1320–1324.

Kraft, M. D., and Greeley, R. 2000. Rock coatings and aeolian abrasion on Mars: application to the Pathfinder landing site. J. Geophys. Res. 105(E6):15107–15116.

Krauskopf, K. B. 1957. Separation of manganese from iron in sedimentary processes. Geochim. Cosmochim. Acta 12:61–84.

Krinsley, D. 1998. Models of rock varnish formation constrained by high resolution transmission electron microscopy. Sedimentology 45:711–725.

Krinsley, D.; Ditto, J.; Langworthy, K.; Dorn, R. I.; and Thompson, T. 2013. Varnish microlaminations: new insights from focused ion beam preparation. Phys. Geogr. 34:159–173.

Krinsley, D.; Dorn, R. I.; and DiGregorio, B. 2009. Astrobiological implications of rock varnish in Tibet. Astrobiology 9:551–562.

Krinsley, D.; Dorn, R. I.; and Tovey, N. K. 1995. Nanometer-scale layering in rock varnish: implications for genesis and paleoenvironmental interpretation. J. Geol. 103:106–113.

Krinsley, D., and Rusk, B. G. 2000. Bacterial presence in layered rock varnish—possible Mars analog? *In* 2nd International Conference on Mars Polar Science and Exploration. http://www.lpi.usra.edu/meetings/polar2000/pdf/4001.pdf.

Krinsley, D. H.; Dorn, R. I.; DiGregorio, B. E.; Langworthy, K. A.; and Ditto, J. 2012. Rock varnish in New York: an accelerated snapshot of accretionary processes. Geomorphology 138:339–351.

Krumbein, W. E. 1969. Über den Einfluss der Mikroflora auf die exogene Dynamik (Verwitterung und Krustenbildung). Geol. Rundsch. 58:333–363.

Krumbein, W. E., and Jens, K. 1981. Biogenic rock varnishes of the Negev Desert (Israel): an ecological study of iron and manganese transformation by cyanobacteria and fungi. Oecologia 50:25–38.

Kuhlman, K. R.; Allenbach, L. B.; Ball, C. L.; Fusco, W. G.; La Duc, M. T.; Kuhlman, G. M.; Anderson, R. C.; et al. 2005. Enumeration, isolation, and characterization of ultraviolet (UV-C) resistant bacteria from rock varnish in the Whipple Mountains, California. Icarus 174:585–595.

Kuhlman, K. R.; Fusco, W. G.; La Duc, M. T.; Allenbach, L. B.; Ball, C. L.; Kuhlman, G. M.; Anderson, R. C.; et al. 2006*a*. Diversity of microorganisms within rock varnish in the Whipple Mountains, California. Appl. Environ. Microbiol. 72:1708–1715.

Kuhlman, K. R.; McKay, C. P.; Venkat, P.; La Duc, M. T.; Kuhlman, G. M.; and Principe, E. 2006*b*. Microbial fauna associated with rock varnish at Yungay, Atacama Desert, Chile. Astrobiology 6:153–154.

Kuhlman, K. R.; Venkat, P.; La Duc, M. T.; Kuhlman, G. M.; and McKay, C. P. 2008. Evidence of a microbial community associated with rock varnish at Yungay, Atacama Desert, Chile. J. Geophys. Res. 113:G04022. doi:10.1029/2007JG000677.

Labrenz, M. 2004. Living science: Peter Hirsch celebrates his 75th birthday. Microb. Ecol. 47:197–199.

Lanza, N. L.; Fischer, W. W.; Wiens, R. C.; Grotzinger, J.; Ollila, A. M.; Cousin, A.; Anderson, R. B.; et al. 2014. High manganese concentrations in rocks at Gale crater, Mars. Geophys. Res. Lett. 41:5755–5763.

Larsen, E. I.; Sly, L. I.; and McEwan, A. G. 1999. Manganese(II) adsorption and oxidation by whole cells and a membrane fraction of *Pedomicrobium* sp. ACM 3067. Arch. Microbiol. 171:257–264.

Larson, P. H., and Dorn, R. I. 2012. Painting Yosemite Valley: a case study of rock coatings encountered at Half Dome. Phys. Geogr. 33:165–182.

Learman, D. R.; Wankel, S. D.; Webb, S. M.; Martinez, N.; Madden, A. S.; and Hansel, C. M. 2011. Coupled biotic-abiotic Mn(II) oxidation pathway mediates the formation and structural evolution of biogenic Mn oxides. Geochim. Cosmochim. Acta 75:6048–6063.

Linck, G. 1900. Über die dunkel Rinden der Gesteine der Wüsten. Jena. Z. Natwiss. 35:1–8.

Liu, T., and Broecker, W. S. 2000. How fast does rock varnish grow? Geology 28:183–186.

———. 2008. Rock varnish microlamination dating of late Quaternary geomorphic features in the drylands of the western USA. Geomorphology 93:501–523.

———. 2013. Millennial-scale varnish microlamination dating of late Pleistocene geomorphic features in the drylands of western USA. Geomorphology 187:38–60.

Lozano, R. P., and Rossi, C. 2012. Exceptional preservation of Mn-oxidizing microbes in cave stromatolites (El Soplao, Spain). Sediment. Geol. 255–256:42–55.

Lucas, A. 1905. The blackened rocks of the Nile cataracts and of the Egyptian deserts. Cairo, National Printing Department.

Macholdt, D. S.; Jochum, K. P.; Pöhlker, C.; Stoll, B.; Weis, U.; Weber, B.; Müller, M.; et al. 2015. Microanalytical methods for in-situ high-resolution analysis of rock varnish at the micrometer to nanometer scale. Chem. Geol. 411:57–68.

Madden, A. S., and Hochella, M. F. 2005. A test of geochemical reactivity as a function of mineral size: manganese oxidation promoted by hematite nanoparticles. Geochim. Cosmochim. Acta 69:389–398.

McKeown, D. A., and Post, J. E. 2001. Characterization of manganese oxide mineralogy in rock varnish and dendrites using X-ray absorption spectroscopy. Am. Mineral. 86:701–713.

MEPAG (Mars Exploration Program Analysis Group). 2015. Mars science goals, objectives, investigations, and priorities: 2015 version. http://mepag.nasa.gov /reports/MEPAG%20Goals_Document_2015_v5.pdf. Washington, DC, National Aeronautics and Space Administration.

Ming, D. W.; Mittlefehldt, D. W.; Gellert, R.; Peretyazhko, T.; Clark, B. C.; Morris, R. V.; Yen, A. S.; et al. 2015. Iron-manganese redox reactions in Endeavour Crater rim apron rocks. In 46th Lunar and Planetary Science Conference. http://www.hou.usra.edu/meetings/lpsc2015 /pdf/2676.pdf.

Nagy, B.; Nagy, L. A.; Rigali, M. J.; Jones, W. D.; Krinsley, D. H.; and Sinclair, N. 1991. Rock varnish in the Sonoran Desert: microbiologically mediated accumulation of manganiferous sediments. Sedimentology 38:1153–1171.

Nealson, K. H. 2006. The manganese-oxidizing bacteria. Prokaryotes 57:222–231.

Nealson, K. H., and Tebo, B. 1980. Structural features of manganese precipitating bacteria. In Ponnamperuma,

C., and Margulis, L., eds. Limits of life. Dordrecht, Reidel, p. 173–182.

Northrup, D. E.; Barns, S. M.; Yu, L. E.; Spilde, M. N.; Schelble, R. T.; Dano, K. E.; Crossey, L. J.; et al. 2003. Diverse microbial communities inhabiting ferromanganese deposits in Lechuguilla and Spider Caves. Environ. Microbiol. 5:1071–1086.

Northup, D. E.; Snider, J. R.; Spilde, M. N.; Porter, M. L.; van de Kamp, J. L.; Boston, P. J.; Nyberg, A. M.; and Bargar, J. R. 2010. Diversity of rock varnish bacterial communities from Black Canyon, New Mexico. J. Geophys. Res. 115:G02007. doi:10.1029/2009JG001107.

Nowinski, P.; Hodge, V. F.; Lindley, K.; and Cizdziel, J. V. 2010. Elemental analysis of desert varnish samples in the vicinity of coal-fired power plants and the Nevada Test Site using laser ablation ICP-MS. Open Chem. Biomed. Methods J. 3:153–168.

Palmer, F. E.; Staley, J. T.; Murray, R. G. E.; Counsell, T.; and Adams, J. B. 1985. Identification of manganese-oxidizing bacteria from desert varnish. Geomicrobiol. J. 4:343–360.

Percy, J. W. 1993. The Erie Canal: from Lockport to Buffalo. Buffalo, Western New York Heritage Institute of Canisius College.

Perry, R. S.; Dodsworth, J.; Staley, J. T.; and Engel, M. H. 2004a. Bacterial diversity in desert varnish. In Mars: the search for life. Proceedings of the III European Workshop on Exo/Astrobiology. Noordwijk, Netherlands, European Space Agency, p. 259–260.

Perry, R. S.; Engel, M.; Botta, O.; and Staley, J. T. 2003. Amino acid analyses of desert varnish from the Sonoran and Mojave Deserts. Geomicrobiol. J. 20:427–438.

Perry, R. S.; Gorbushina, A. A.; Engel, M. H.; Kolb, V. M.; Krumbein, W. E.; and Staley, J. T. 2004b. Accumulation and deposition of inorganic and organic compounds by microcolonial fungi. In Mars: the search for life. Proceedings of the III European Workshop on Exo/Astrobiology. Noordwijk, Netherlands, European Space Agency, p. 55–58.

Perry, R. S., and Kolb, V. M. 2003. Biological and organic constituents of desert varnish: review and new hypotheses. In Hoover, R. B., and Rozanov, A. Y., eds. Instruments, methods, and missions for astrobiology VII. Proc. SPIE 5163:202–217. doi:10.1117/12.509695.

Potter, R. M. 1979. The tetravalent manganese oxides: clarification of their structural variations and relationships and characterization of their occurrence in the terrestrial weathering environment as desert varnish and other manganese oxides. PhD dissertation, California Institute of Technology, Pasadena.

Potter, R. M., and Rossman, G. R. 1977. Desert varnish: the importance of clay minerals. Science 196:1446–1448.

———. 1978. Manganese oxides in the terrestrial weathering environment [abs.]: Geol. Soc. Am. Abstr. Program 10:473.

———. 1979a. The manganese- and iron-oxide mineralogy of desert varnish. Chem. Geol. 25:79–94.

———. 1979b. Mineralogy of manganese dendrites and coatings. Am. Mineral. 64:1219–1226.

———. 1979c. The tetravalent manganese oxides: identification, hydration, and structural relationships by infrared spectroscopy. Am. Mineral. 64:1199–1218.

Probst, L. W.; Allen, C. C.; Thomas-Keprta, K. L.; Clemett, S. J.; Longazo, T. G.; Nelman-Gonzalez, M. A.; and Sams, C. 2002. Desert varnish—preservation of biofabrics and implications for Mars. In 33rd Lunar and Planetary Science Conference. http://www.lpi.usra.edu/meetings/lpsc2002/pdf/1764.pdf.

Richie, N. W. M. 2013. DTSA-II and EPQ library. Material Measurement Laboratory. http://www.cstl.nist.gov/div837/837.02/epq/dtsa2/index.html. Accessed April 2, 2013.

Schelble, R.; McDonald, G.; Hall, J.; and Nealson, K. 2005. Community structure comparison using FAME analysis of desert varnish and soil, Mojave Desert, California. Geomicrobiol. J. 22:353–360.

Skoog, D. A.; Holler, F. J.; and Crouch., S. R. 2007. Principles of instrumental analysis (6th ed.). Salt Lake City, UT: Brooks Cole.

Soleilhavoup, F. 2011. Microformes d'accumulation et d'ablation sur les surfaces désertiques du Sahara. Geomorphol. Relief Processus Environ. 2:173–186.

Spilde, M. N.; Melim, L. A.; Northrup, D. E.; and Boston, P. J. 2013. Anthropogenic lead as a tracer for rock varnish growth: implications for rates of formation. Geology 41:263–266.

Staley, J. T.; Adams, J. B.; and Palmer, F. E. 1991. Desert varnish: a biological perspective. Soil Biochem. 7:173–195.

Staley, J. T.; Jackson, M. J.; Palmer, F. E.; Adams, J. C.; Borns, D. J.; Curtiss, B.; and Taylor-George, S. 1983. Desert varnish coatings and microcolonial fungi on rocks of the Gibson and Great Victoria Deserts, Australia. BMR J. Aust. Geol. Geophys. 8:83–87.

Sterflinger, K.; Krumbein, W. E.; Lallau, T.; and Rullkötter, J. 1999. Microbially mediated orange patination of rock surfaces. Anc. Biomol. 3:51–65.

Taylor-George, S.; Palmer, F. E.; Staley, J. T.; Borns, D. J.; Curtiss, B.; and Adams, J. B. 1983. Fungi and bacteria involved in desert varnish formation. Microb. Ecol. 9:227–245.

Tebo, B. M.; Bargar, J. R.; Clement, B. G.; Dick, G. J.; Murray, K. J.; Parker, D.; Verity, R.; and Webb, S. M. 2004. Biogenic manganese oxides: properties and mechanisms of formation. Annu. Rev. Earth Planet. Sci. 32:287–328.

Tebo, B. M.; Johnson, H. A.; McCarthy, J. K.; and Templeton, A. S. 2005. Geomicrobiology of manganese(II) oxidation. Trends Microbiol. 13:421–428.

Tyler, P. A., and Marshall, K. C. 1967a. Form and function in manganese-oxidizing bacteria. Arch. Mikrobiol. 56:344–353.

———. 1967b. Microbial oxidation of manganese in hydro-electric pipelines. Antonie Leeuwenhoek 33:171–183.

van Waasbergen, L. G.; Hildebrand, M.; and Tebo, B. M. 1996. Identification and characterization of a gene cluster involved in manganese oxidation by spores of the marine Bacillus sp. strain SG-1. J. Bacteriol. 178:3517–3530.

Viles, H. A. 1995. Ecological perspectives on rock surface weathering: towards a conceptual model. Geomorphology 13:21–35.

Villalobos, M.; Toner, B.; Bargar, J.; and Sposito, G. 2003. Characterization of the manganese oxide produced by Pseudomonas putida strain MnB1. Geochim. Cosmochim. Acta 67:2649–2662.

von Humboldt, A. 1812. Personal narrative of travels to the equinoctial regions of America during the years 1799–1804 by Alexander von Humboldt and Aimé Bonpland. Vol. 2. Ross, T., transl. and ed. London, George Bell.

Wang, X.; Zeng, L.; Wiens, M.; Schloßmacher, U.; Jochum, K. P.; Schröder, H. C.; and Müller, W. E. G. 2011. Evidence for a biogenic, microorganismal origin of rock varnish from the Gangdese Belt of Tibet. Micron 42:401–411.

Warscheid, T. 1990. Untersuchungen zur Biodeterioration von Sandsteinen unter besonderer Berücksichtigung der chemoorganotrophen Bakterien. PhD dissertation, University of Oldenburg.

Whalley, W. B. 1983. Desert varnish. In Goudie, A. S., and Pye, K., eds. Chemical sediments and geomorphology: precipitates and residua in the near-surface environment. London, Academic Press, p. 197–226.